Environmental Science and Pollution Research (2019) 26:3262–3291
https://doi.org/10.1007/s11356-018-3884-z

REVIEW ARTICLE

Synthesis and applications of nano-TiO_2: a review

Muhammad Tayyab Noman[1] · Muhammad Azeem Ashraf[2] · Azam Ali[1]

Received: 5 September 2018 / Accepted: 27 November 2018 / Published online: 6 December 2018

Abstract

TiO_2-based nanomaterials have attracted prodigious attention as a photocatalysts in numerous fields of applications. In this thematic issue, the mechanism behind the photocatalytic activity of nano-TiO_2 as well as the critical properties have been reviewed in details. The synthesis routes and the variables that affect the size and crystallinity of nano-TiO_2 have also been discussed in detail. Moreover, a newly emerged class of color TiO_2, TiO_2 in aerogel form, nanotubes form, doped and undoped form, and other forms of TiO_2 have been discussed in details. Photocatalytic and photovoltaic applications and the type of nano-TiO_2 that is more suitable for these applications have been discussed in this review.

Keywords Nano-TiO_2 · Photocatalysis · Photovoltaic · Nanocomposites · DSSC

Abbreviations

NPs	Nanoparticles
NMs	Nanomaterials
SEM	Scanning electron microscopy
EDX	Energy dispersive X-ray spectroscopy
TTC	Titanium tetrachloride
TTIP	Titanium tetraisopropoxide
EG	Ethylene glycol
MB	Methylene blue
TEM	Transmission electron microscopy
TiO_2	Titanium dioxide, titania
RNP	Resulting nanoparticles
XRD	X-ray diffractometry
UV	Ultraviolet
nm	Nanometer
mL	Milliliter
h	Hour
°C	Degree Celsius
K	Kelvin
MPa	Megapascals
Ks^{-1}	Kelvin per second
mj m^{-2}	Millijoule per square meter
$TiCl_4$	Titanium tetrachloride
$m^2\ g^{-1}$	Meter square per gram
eV	Electron volts
$OH^{\cdot}$	Hydroxyl radical
$^{\cdot}O_2^-$	Super oxide anion
Ti	Titanium
°	Degree
S. aureus	*Staphylococcus aureus*
E. coli	*Escherichia coli*
JCPDS	Joint Committee on Powder Diffraction Standards
N_2	Nitrogen dioxide
CO_2	Carbon dioxide
COD	Chemical oxygen demand
ROS	Reactive oxygen species
IR	Infrared
3D	Three dimensional
2D	Two dimensional
V	Volts
EPR	Electron paramagnetic resonance
TNTs	TiO_2 nanotubes
TEOH	Triethanol amine
pH	Power of hydrogen
C. albicans	*Candida albicans*
MO	Methyl orange
RB	Rhodamine B

Responsible editor: Suresh Pillai

✉ Muhammad Tayyab Noman
tayyab_noman411@yahoo.com

[1] Department of Material Engineering, Technical University of Liberec, Liberec, Czech Republic

[2] Department of Fibre and Textile Technology, University of Agriculture, Faisalabad, Pakistan

HRTEM	High-resolution transmission electron microscope
CHFS	Continuous hydrothermal flow synthesis
FTO	Fluorine-doped tin oxide
AFM	Atomic force microscopy
TENOH	Tetraethylammonium hydroxides
TANOH	Tetraalkylammonium hydroxides
Ag	Silver
Fe	Ferric
Au	Gold
TBNOH	Tetrabutylammonium hydroxides
NaOH	Sodium hydroxide
P25	Commercially available TiO_2
EN	Ethylenediamine
FSP	Flame spray pyrolysis
TGA-DTA	Thermogravimetric-differential thermal analysis
Cu	Copper
BTCA	Butane tetracarboxylic acid
CA	Citric acid
NDMA	N-Nitrosodimethylamine
DSSC	Dye-sensitized solar cell
QDSSC	Quantum dot-sensitized solar cell
DSPC	Dye-sensitized photoelectrochemical cell
FTIR	Fourier transform infrared spectroscopy
η_{SUN}	Solar light-to-power conversion efficiency
J_{SC}	Short-circuit photocurrent

Introduction

During past few decades, TiO_2 (titanium dioxide, titania) has been widely researched and used in numerous fields under diverse applications ranges from sunscreens to photovoltaic cell. This happens because of its physicochemical properties, i.e., absorption of ultraviolet (UV) light and higher refractive index which enables TiO_2 to work as a multifunction material. The essential applications of TiO_2 such as photocatalytic degradation and splitting, photovoltaic cells, electrochromic devices, hydrogen storage, and sensing instruments have encouraged massive interest and extensive advancement in the synthesis of TiO_2 NMs (nanomaterials) in the last few years (Chen et al. 2012; Chen and Mao 2007; Fujishima et al. 2000; Henderson and Lyubinetsky 2013; Pang et al. 2013; Schneider et al. 2014; Thompson and Yates 2006; Zhang and Yates 2012). The main objective of this thematic study is to demonstrate a comprehensive review on the synthesis and applications of TiO_2 NMs that can provide a complete information about this interesting material to newcomers and experienced researchers as a valuable reference in research field. During the last years, many review papers have been published on TiO_2, i.e., He and Chen reviewed the properties of nano-TiO_2 and analyzed its role in photodegradation of organic pollutants. They also explained the effects of doping, surface modifications, synthesis techniques, and many other operational parameters (He and Chen 2012). But we still believe that this approach is unique one in its scope and it provides a complete image for synthesis and applications of TiO_2 NMs. It looks pretty reasonable to assume that this review will stimulate new concepts in different research related areas.

The following articles describe the theoretical and experimental studies regarding principle physicochemical properties of different TiO_2 NMs. In some cases, bulk TiO_2 is considered as a reference. Zhang and Banfield explained thermodynamic, mechanical, and structural properties of TiO_2 NMs which involved numerous crystalline phases, phase stability, dislocations, contraction, and expansion of lattice parameters as illustrated in Fig. 1 (Zhang and Banfield 2014). Coppens et al. reported a brief overview on the properties and crystal morphologies of polyoxotitanate nanoclusters that involved chromophore attachment (Coppens et al. 2014). Kapilashrami et al. reviewed electronic and optical properties of TiO_2 NPs (nanoparticles). They discussed the doping effect and explained the correlation among optical and electronic properties of TiO_2 NMs with their crystal facets (Kapilashrami et al. 2014).

In another article regarding the properties of TiO_2 NMs, Angelis et al. discussed theoretical studies of bulk and nano-TiO_2. They presented the optical and electronic properties of anatase TiO_2 in bulk and nanoforms, modeling of TiO_2 NPs, nanotubes, and nanosheets in their bare and sensitized forms (De Angelis et al. 2014). Bourikas et al. presented the solid-liquid interfacial chemistry of rutile and anatase crystals of TiO_2 and deposition of catalysts on their surfaces. They summarize the surface chemistry by TiO_6 octahedron distortion between anatase and rutile, difference between lattice parameters and space group as illustrated in Fig. 2 (Bourikas et al. 2014). The synthesis methods used for the fabrication of NMs have a significant effect on the dimensions of NMs. Overall, NMs vary from 0 to 3 in dimensions and normally different NMs are recognized by specific dimensions such as spherical NPs have zero dimension; nanorods, nanowires, nanotubes, and nanobelts have one dimension; nanosheets have two dimensions; and porous nanostructures have three-dimensional structures. Sang et al. described synthesis, characterization, and charge separation properties of zero dimensional TiO_2 NPs (Sang et al. 2014). Solution-based synthesis of TiO_2 NPs is reported by Cargnello et al. They designed fundamentals for synthesis of TiO_2 NPs and proposed the effect of different precursors under aqueous, non-aqueous, and templated methods for producing TiO_2 NPs (Cargnello et al. 2014). Wang et al. reported one-dimensional TiO_2 nanostructures, i.e., nanorods, nanobelts, and nanowires. They discussed and summed up different growth mechanisms like solid-liquid-vapor and vapor-based synthesis, oriented attachment, evaluated different solutions, and described a detailed

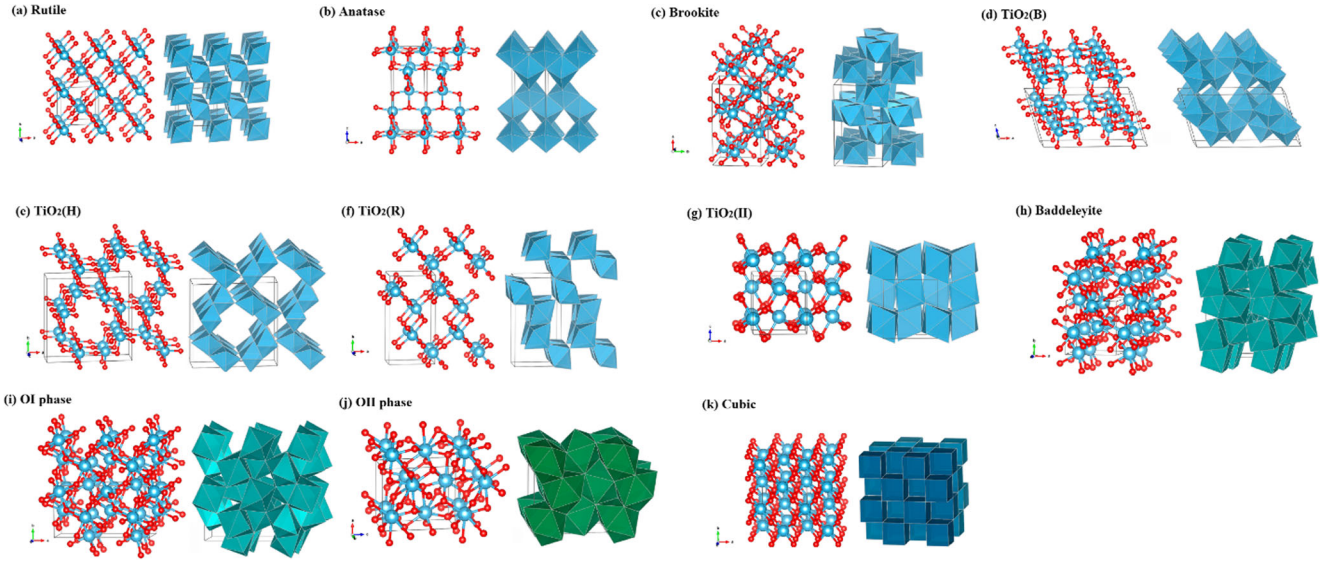

Fig. 1 Structures of different TiO_2 phases. **a** Rutile, **b** anatase, **c** brookite, **d** TiO_2(B), **e** TiO_2(H), **f** TiO_2(R), **g** TiO_2(II), **h** baddeleyite phase, **i** OI phase, **j** OII phase **k** cubic phase. Reprinted with permission from Zhang and Banfield (2014). Copyright 2014, with permission from the American Chemical Society

thematic picture of the properties and applications of these NMs in energy storage and photovoltaics (Wang et al. 2014c).

In another review article, Lee et al. added another important type in one-dimensional TiO_2 family, i.e., nanotubes. They summarized their growth mechanisms; electronic, optical, and structural properties; and applications in electrical, optoelectronic, and biomedical areas (Lee et al. 2014). Wang and Sasaki reviewed the two-dimensional nanosheets of TiO_2 and elaborate the synthesis methods and properties of up given nanosheets, summarized the mechanisms of designing complex structures created by two-dimensional nanosheets, and presented their applications in different fields, i.e., photocatalytic, photochemical, dielectric, biomedical, and electrochemical (Wang and Sasaki 2014). Fattakhova et al. reported a detail article on the synthesis of three-dimensional porous nanostructures. They summarized different synthesis methods for developing TiO_2 nanoporous films, porous fibers, porous spheres, and ordered hollow spheres, etc. (Fattakhova-Rohlfing et al. 2014). The development of TiO_2 nanocrystals with specific facets is a crucial concept in recent literature. Liu et al. reported a comprehensive review on the up given theme. They sum up the primary methods to synthesize the crystals of rutile, anatase, and brookite and explained the exceptional electronic, structural, and absorption properties of various facets. Anatase and rutile crystals' shape at equilibrium are illustrated in Fig. 3 (Liu et al. 2014a).

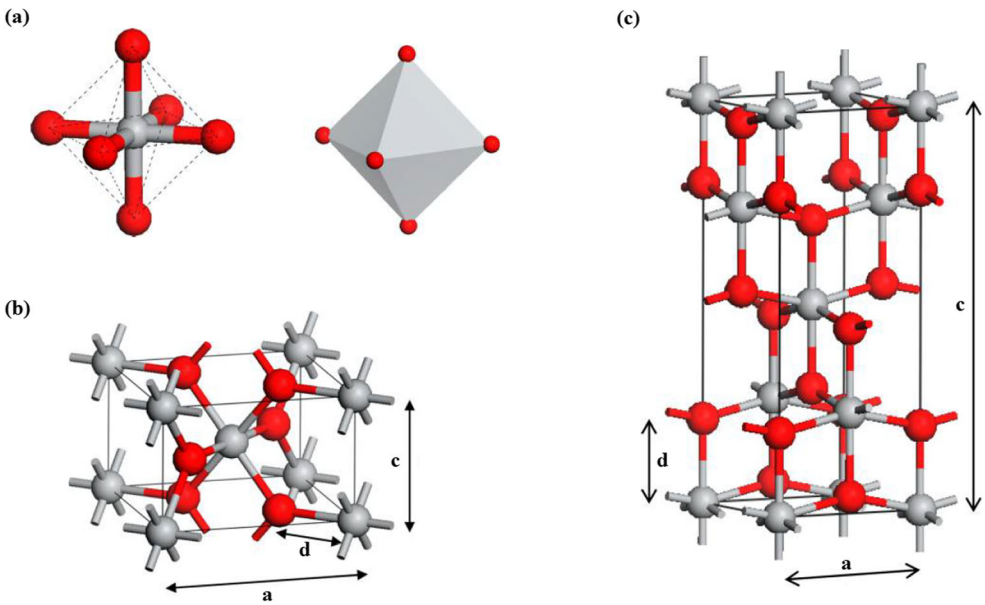

Fig. 2 **a** Schematic representation of the distorted TiO_6 octahedron of TiO_2 (anatase and rutile). **b** Tetragonal structure of rutile described by using two cell edge parameters, (a) and (c), and one internal parameter, (d). **c** Tetragonal structure of anatase described by using two cell edge parameters, (a) and (c), and one internal parameter, (d). Reprinted with permission from Bourikas et al. (2014)). Copyright 2014, with permission from the American Chemical Society

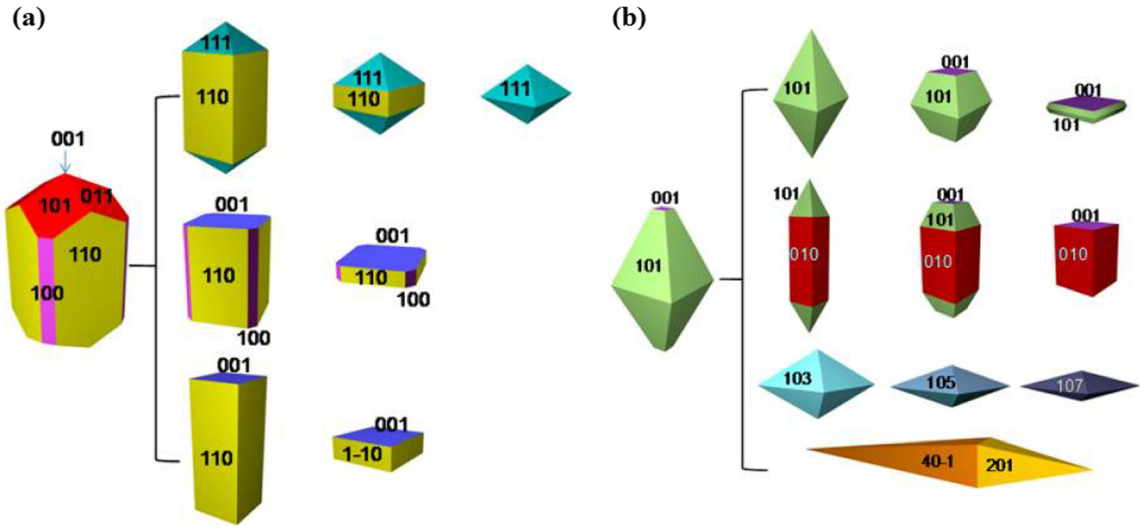

Fig. 3 Equilibrium crystal shapes of TiO_2 through the Wulff construction, (**a**) rutile and (**b**) anatase. Reprinted with permission from Liu et al. (2014a)). Copyright 2014, with permission from the American Chemical Society

To increase performance of TiO_2 NMs, structural modifications have been done by different techniques such as doping, compositing, and self-structured modifications. Doping with non-metals has gained considerable attraction in the last few years as it reduces the absorption threshold to visible light region. Asahi et al. reported an overview on N_2-doped TiO_2 NMs. They sum up the synthesis of nitrogen-doped TiO_2 NMs, strategies for absorption of visible light, and their utilization in interior, textile, water, and air purification (Asahi et al. 2014). Dahl et al. presented the modified TiO_2 NMs by developing composites with metal oxides, metals, semiconductors, and carbon nanostructures. The development of a heterojunctions between TiO_2 and other materials is one of the major advantages of this technique that favors the separation of photoexcited charge carriers. They reported that photocatalytic process occurs in three steps: (i) absorption of photons on the surface to produce electron-hole pairs, (ii) separation of charge carriers and migration towards the surface, and (iii) redox reactions with adsorbed reactants. The mechanism of photocatalysis on the surface of bare and composite TiO_2 is illustrated in Fig. 4 (Dahl et al. 2014). Recently, Liu and Chen presented a hot topic on the modifications induced by self-structured alterations. They summarized lattice defects, strain, lattice deformation in hydrogenated and amorphous phases, and property changes in the hydrogenated phases with concerned physical and chemical features (Liu and Chen 2014).

The applications of TiO_2 NMs range from photocatalysis to bio-sensing. Schneider et al. observed the effects of TiO_2-based photocatalysis on environmental applications. They sum up time-resolved analysis, the synthesis of doped TiO_2 NPs, photoinduced surface changes, and visible light reactive thin films (Schneider et al. 2014). Ma et al. examined the photocatalytic fuel generation applications of TiO_2 NMs and summarized the various aspects regarding photocatalytic hydrogen production from splitting of water, photocatalytic reduction of CO_2 into fuels, along with the influences of reaction mechanisms and reaction conditions (Ma et al. 2014). Liu et al. discussed the influence of bioinspired nano-TiO_2 with special wettability and summarized fundamental theories about super hydrophobic, super hydrophilic, and super oleophobic TiO_2 surfaces and their antimicrobial, antifogging, self-cleaning, anticorrosion, water condensation, and biomedical applications (Liu et al. 2014b). Bai et al. reported a detail overview on the role of TiO_2 NMs for photovoltaic applications and summarized the fundamental theories about surface treatments in different kinds of solar cells, their organic-inorganic interactions, and charge carrier transport and their recombination (Bai et al. 2014). For sensor applications such as biosensors, gas sensors, and COD (chemical oxygen demand) sensors, TiO_2 NMs have been reviewed by Bai and Zhou (2014). Rajh et al. explained a comparatively new concept of TiO_2 NMs in biomedical applications. They focussed on the importance of ROS (reactive oxygen species), phototoxicity, TiO_2-protein hybrid, nanoparticles redox active centers, TiO_2-DNA hybrid, imaging guided therapy, surface sites, and drug delivery (Rajh et al. 2014).

Colfen and Antonietti reviewed the mesocrystallization forms of inorganic structures developed by self-controlled crystallization that follow nanobuilding block strategy that gives a more independent crystallization which provides new openings for crystallization morphologies (Cölfen and Antonietti 2005). In recent years, a newly emerged class of colored, i.e., black, blue, brown, red, TiO_2 nanostructures has been reported by different researchers. Ullattil et al. recently reported a class of colored TiO_2 nanomaterials consisting of black TiO_2 that helps to maximize the solar energy absorption from UV to IR by improving optical properties of TiO_2 (Ullattil et al. 2018). Ullattil and periyat developed a one pot

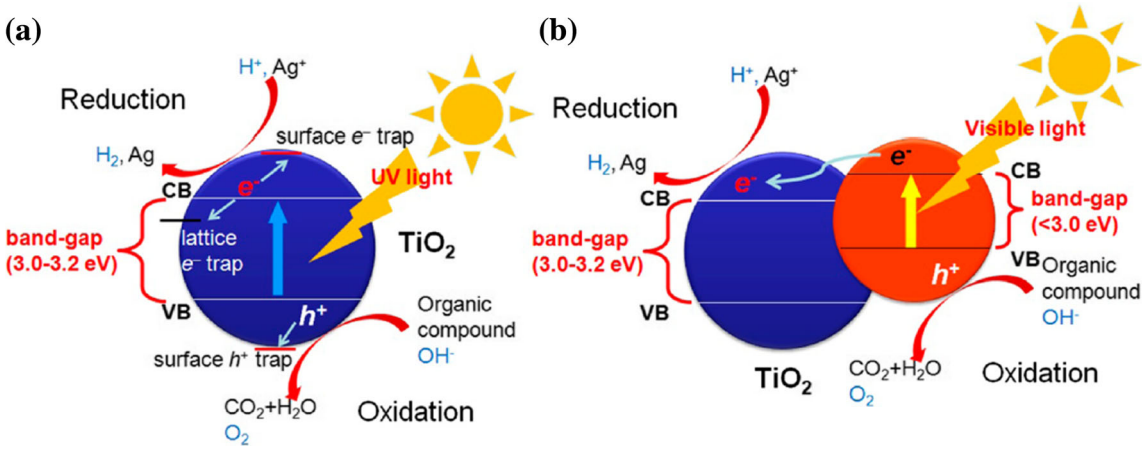

Fig. 4 General model of photocatalysis of **a** bare TiO_2 and **b** composite TiO_2 exhibiting a heterojunction and charge trapping on TiO_2 and the second component. Reprinted with permission from Dahl et al. (2014)). Copyright 2014, with permission from the American Chemical Society

gel combustion method for the synthesis of self-doped black anatase TiO_2 that enhanced 33% more photocatalytic efficiency than P25 (Ullattil and Periyat 2016). In a previous investigation, Ullattil and Periyat developed black and yellow TiO_2 NPs in their anatase form through a rapid green microwave method in which Mn (II) was used as a phase purifier (Ullattil and Periyat 2015).

Properties of nano-TiO_2

Among all other semiconductor metal oxides family, TiO_2 NMs have gained much appreciation and seems to be a distinctive candidate due to their high structural, electronic and optical stability, nontoxicity, corrosion resistance, and low cost. TiO_2 has three natural polymorphs commonly known as rutile, anatase, and brookite. The available literature indicates that brookite is more difficult to synthesize, so rarely studied.

Figure 5 describes the unit cell structures for rutile and anatase TiO_2 respectively (Diebold 2003). Both rutile and anatase TiO_2 have tetragonal crystal structure linked by a chain of TiO_6 octahedra, i.e., each unit cell contains six oxygen atoms around one Ti atom. The crystal structures discussed above are different in assembly pattern of their octahedra chains and by distortion of their octahedron. In rutile TiO_2, TiO_6 octahedron exhibits an irregular orthorhombic distortion while it exhibits its symmetry lower than orthorhombic in anatase. Moreover, each octahedron is connected with ten neighboring octahedrons in rutile structure, from which two octahedrons share edges oxygen pairs and eight share corners oxygen atoms but in anatase, each octahedron is connected with eight neighboring octahedrons from which four share an edge and four share a corner respectively. Furthermore, Ti–O distances are larger in rutile than those in anatase while Ti–Ti distances are shorter in rutile structure. These differences in octahedron arrangement make the crystal structures of the up given polymorphs different by changing electronic band structures and mass densities of the two forms of TiO_2.

Barnard et al. reported phase stability of TiO_2 NPs by a thermodynamic model in different environments by performing a series of theoretical studies. They summarized that surface passivation has a crucial effect on phase stability and morphology of nanocrystals and concluded that surface hydrogenation triggers significant changes in rutile nanocrystals. The results also explained that size of rutile nanocrystal drastically increased when surface undercoordinated titanium atoms is H-terminated. The crossover point for spherical NPs is 2.6 nm. They also reported that anatase is more stable than rutile phase below crossover point (Barnard and Zapol 2004). Their study about TiO_2 NPs in water environments reported that transition size is larger in water than that under vacuum. They summarized transition enthalpy of rutile and anatase nanocrystals and concluded that thermochemical results for different facets could be different for size and shape of these nanocrystals. They explained that the size of TiO_2 NPs under varying pH conditions increased from 7 to 23 nm. The shape of the TiO_2 NPs is also changed as described in Fig. 6 (Barnard and Curtiss 2005).

Direct interband transition of electron in pure semiconductors is the core mechanism for light absorption. In indirect semiconductors such as TiO_2, this absorption phenomenon is very small because the crystal symmetry of such semiconductors could not allow the direct electron transitions among the band centers. Braginsky and Shklover described the light absorption enrichment in the crystallites of TiO_2 by momentum non-conservation with indirect electron transitions at the interface. When the interfacial atoms have a larger share, this effect increases at the interface. Moreover, electron's density of states and a large dipole matrix element are responsible for indirect electron transitions. This expected light absorption enrichment is considerable in nanocrystalline TiO_2 as well as microcrystalline and in porous semiconductors only when the

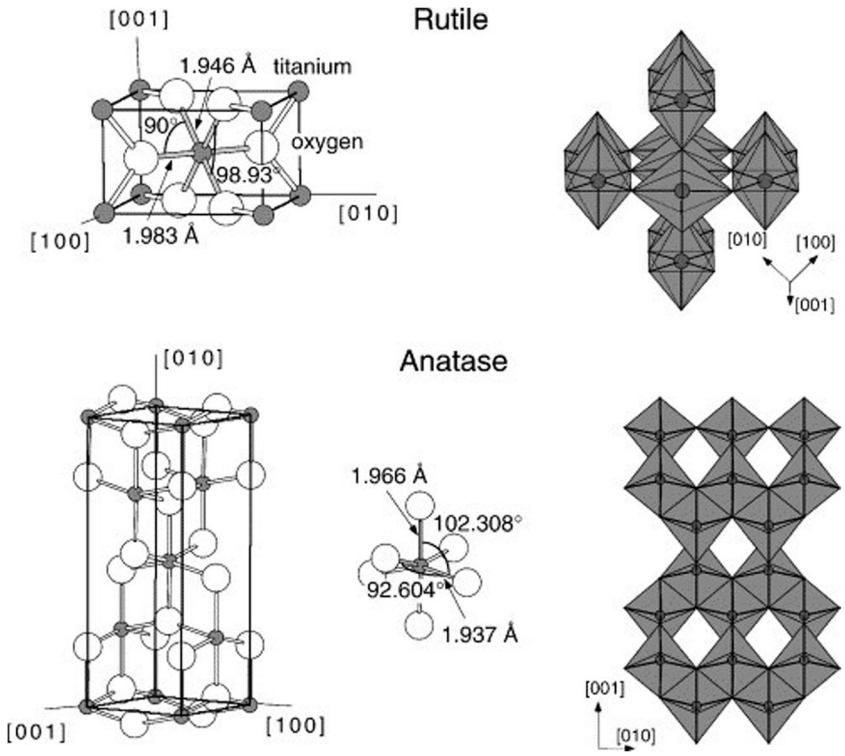

Fig. 5 Rutile and anatase unit cell structures. Reprinted with permission from Diebold (2003)). Copyright 2003, with permission from Elsevier

interfacial atoms have large share. At low photon energy, i.e., hυ < Eg + Wc, a fast increase takes place in light absorption and at any given point in conduction band, electron transitions are only possible when hυ = Eg + Wc, in which Wc refers to conduction band width. The further increase in the absorption is due to the increment in the electron density in valance band. So, the absorption interface becomes the backbone for light absorption for smaller crystallite having size less than 20 nm (Braginsky and Shklover 1999).

It is obvious for NMs that band gap energy increment and decrease in size turns the electronic band structure more discrete (Anpo et al. 1987). Quantum mechanical behavior was observed by charge carriers if size of NPs compared to them having same de Broglie's wavelength that led to a number of discrete electronic states (Henglein 1989). But an inconsistency occurs with size for which TiO_2 NMs perform quantization effects. Sakai et al. and Sato et al. calculated band gap of nano- and bulk TiO_2 and concluded that lower dimensionality such as 2D or 3D transitions leads larger band gap to NMs. They found through calculation that for nano-TiO_2, lower edge of conduction band was 0.1 V higher as compared to bulk anatase TiO_2. Electronic band structure and densities of states of TiO_2 are illustrated in Fig. 7 (Sakai et al. 2004; Sato et al. 2003). When the photons of equal or higher energy levels (> 3 eV) strike on the surface of TiO_2 NMs, electrons are released from valence band to unoccupied conduction band

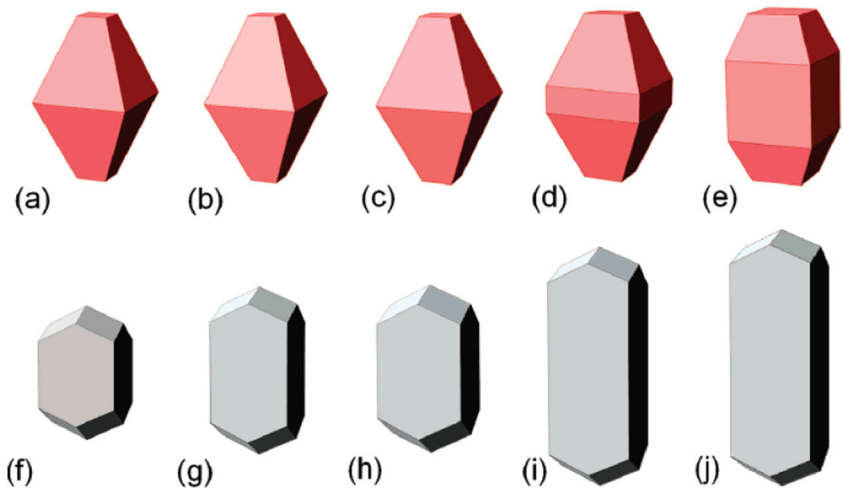

Fig. 6 Morphology predicted for anatase and rutile respectively. **a**, **f** hydrogenated surfaces; **b**, **g** hydrogen-rich surface adsorbates; **c**, **h** hydrated surfaces; **d**, **i** hydrogen-poor adsorbates; and **e**, **j** oxygenated surfaces. Reprinted with permission from Barnard and Curtiss (2005). Copyright 2005, with permission from the American Chemical Society

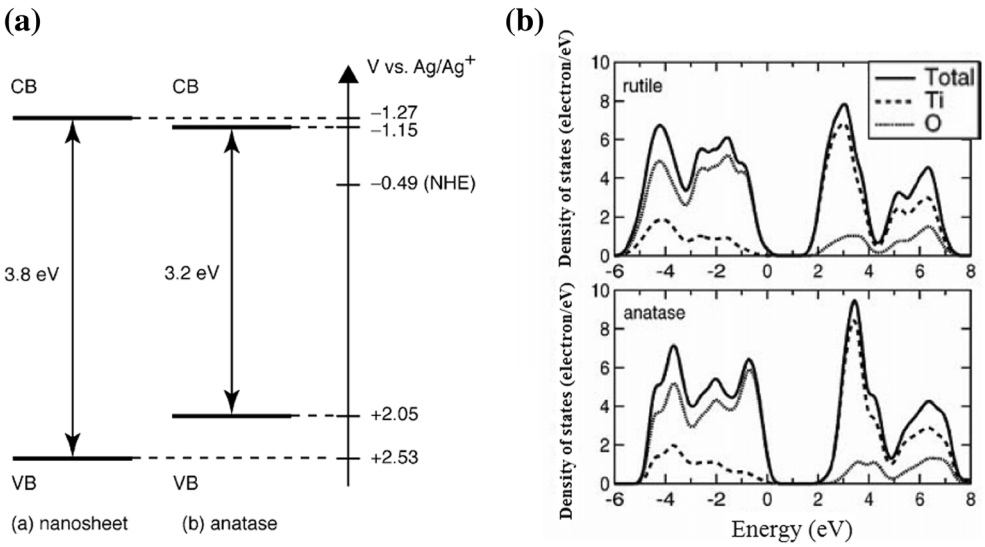

Fig. 7 **a** Electronic band description: (a) TiO_2 nanosheets (b) anatase. Reprinted with permission from Sakai et al. (2004)). Copyright 2004, with permission from the American Chemical Society. **b** Total and partial densities of states for rutile and anatase respectively. Reprinted with permission from Sato et al. (2003)). Copyright 2003, with permission from the American Chemical Society

leaving positive holes in the valance band. These excited electrons and holes are commonly known as charge carriers that try to recombine or may get trapped on the surface and react with absorbed species. The overall output of TiO_2 NMs for different applications is determined by the competition of the following processes (Szczepankiewicz et al. 2000).

Absorption of photon is described in Eq. 1, whereas photocatalytic redox reactions are illustrated in Eqs. 2, 3, 4, 5, and 6, while Eqs. 7, 8, and 9 emphasize on recombination pathways. Equations 3 and 4 explain the reaction mechanisms for holes that lead to attach O vacancies and OH radicals (Szczepankiewicz et al. 2000). The generated charge carriers (electrons, holes) are confined in various defect sites available on the surface of TiO_2 NPs. Hurum et al. reported the results of EPR (electron paramagnetic resonance) that electrons are localized as two Ti^{3+} centers, whereas holes get imprisoned like oxygen-centered radicals linked covalently with surface titanium atoms (Hurum et al. 2005).

$$TiO_2 + h\vartheta \rightarrow e^- + h^+ \quad (1)$$

$$Ti(IV)O{-}H + e^- \rightarrow Ti(III)O{-}H^- \quad (2)$$

$$Ti(IV)O{-}H + h^+ \rightarrow Ti(IV)O^{\cdot}{-}H^+ \quad (3)$$

$$h^+ + {}^1/_2O^{-2}_{lattice} \leftrightarrow {}^1/_4O_2(g) + \text{Vacancy} \quad (4)$$

$$e^- + O_{2,s} \rightarrow O^-_{2,s} \quad (5)$$

$$O^-_{2,s} + H^+ \leftrightarrow HO_{2,s} \quad (6)$$

$$Ti(III)O{-}H^- + h^+ \rightarrow Ti(IV)O{-}H \quad (7)$$

$$Ti(IV)O^{\cdot}{-}H^+ + e^- \rightarrow Ti(IV)O{-}H \quad (8)$$

$$Ti(IV)O^{\cdot}{-}H^+ + O_{2,s} \rightarrow Ti(IV)O{-}H + O_{2,s} \quad (9)$$

Berger et al. investigated electron-hole pair excitations under UV light by EPR and IR (Infrared) spectroscopy for anatase TiO_2 NPs. They found that the electrons trapped at coordinatively unsaturated cations Ti^{3+}, whereas holes (localized states) trapped at oxygen anions which were accessible to EPR spectroscopy. They summarized that the photogenerated electrons get trapped either at localized sites and gave paramagnetic Ti^{3+} centers or remain in conduction band and act as EPR silent species (Berger et al. 2005).

Eskandarloo et al. worked on different morphologies and size uniformity of TiO_2 hollow shells. They used a novel microfluidic droplet-based technique for the fabrication of hollow shells of TiO_2 that further decorated with platinum-based nanostructures which increase their photocatalytic efficiency (Eskandarloo et al. 2018). Afshar et al. synthesized $SrTiO_3$ and TiO_2 NPs with cube, irregular, and some other morphologies under in situ solvothermal and impregnation methods that improvise the charge separation during the photocatalytic redox reactions (Afshar et al. 2016). In another study, Eskandarloo et al. used an ultrasound-assisted sol-gel technique for the synthesis of pure $ZnTiO_3$ and Ce-doped $ZnTiO_3$ novel catalysts that exhibited higher sonocatalytic efficiency than P25 against p-nitrophenol degradation (Eskandarloo et al. 2016). Behnajady and Eskandarloo developed TiO_2 NPs under different pH conditions which give the required crystal phase and crystal size to TiO_2 NPs. They used the artificial neural network for the modeling of photocatalytic efficiency of the developed samples (Behnajady and Eskandarloo 2015). Ultrasonic assisted sol-gel synthesis was used to prepare pure TiO_2, samarium, cerium mono-doped and co-doped TiO_2 by Eskandarloo et al. The developed NPs showed excellent sonocatalytic activity against model organic pollutant, i.e., MO (methyl orange) (Eskandarloo et al. 2015). Hydrothermal treatment was utilized for the preparation of novel TiO_2 nanotubes (TNTs) by Sattarfard et al. These TNTs provide higher adsorption capacity and larger surface area. Basic violet 2 was used as a model pollutant to

investigate the adsorption capacity. Some important operational variables were also investigated and their results were used to analyze the adsorption kinetics and isotherms (Sattarfard et al. 2018). The consumption of electrical energy has been minimized by Eskandarloo et al., in photocatalytic reduction of Cr (VI) to Cr (III) which is considered as an important factor in wastewater treatment. They used Mg and Ag co-impregnated TiO_2 NPs for this study (Eskandarloo et al. 2014). Behnajady et al. prepared stable anatase form of TiO_2 NPs by using sol-gel process under different conditions and at low temperature and investigated the photocatalytic activity of the synthesized samples. They utilized TTIP as a precursor of titanium in their study (Behnajady et al. 2011b). Behnajady et al. investigated the synthesis variables and their effect during a sol-gel process on the structural properties of TiO_2 NPs. Their results showed that the synthesized NPs indicate high photocatalytic performance than commercially available P25 (Behnajady et al. 2011a).

Synthesis of nano-TiO_2

This thematic study enlightens the synthesis methods mostly used in the fabrication of nano-TiO_2 for photocatalytic and photovoltaic applications. Our main aim is to enlighten the scope of sol-gel and hydrothermal and sonochemical methods and their advantages, disadvantages, and research progress.

Sol-gel synthesis

Sol-gel is most versatile method used in fabrication of numerous ceramic materials (Lu et al. 2002; Pierre and Pajonk 2002; Wight and Davis 2002). In a distinctive process, hydrolysis of precursors formed a colloidal suspension named as sol. Precursors used are inorganic metal salts or metal alkoxides. The loss of solvents and completion of polymerization process guide liquid sol to transform itself into solid gel. The sol is cast into a mold to produce gel which further changed itself as a dense ceramic through heating. An aerogel which is known as an extremely low-dense and highly porous material is formed when the solvent is removed in a wet gel form under supercritical conditions. From the sol, ceramic fibers can also be drawn if viscosity is adjusted in an appropriate viscosity range. Uniform and ultrafine powder can be obtained by spray pyrolysis, precipitation, or emulsion processes and NMs can be obtained by using suitable conditions.

Bessekhouad et al. and Znaidi et al. described the synthesis of TiO_2 under sol-gel technique (Bessekhouad et al. 2003; Znaidi et al. 2001). Titanium precursors were hydrolyzed by an acid catalytic step followed by condensation to complete the mechanism. Ti–O–Ti chains growth in the mixture is favored with excess amount of titanium precursors. The growth in Ti–O–Ti chain results in the development of 3D polymeric skeletons with close packed particles. Medium water content with high hydrolysis rates lead the development of Ti $(OH)_4$. The existence of Ti–OH bond in bulk and insufficient growth results loosely packed particles (Anderson et al. 1988; Banfield 1998; Barbé et al. 1997; Choi et al. 1994; Look and Zukoski 1995; O'regan and Gratzel 1991). Oskam et al. studied the growth kinetics in aqueous solution and reported that increase in rate constant of coarsening with increasing temperature is because of equilibrium solubility of TiO_2 and viscosity of the solution. With higher temperatures and longer times, primary particles are transformed into secondary particles by their epitaxial self-assembly. A linear increment in the radius of TiO_2 NPs has a good accord with coarsening model provided by Lifshitz-Slyozov-Wagner (Oskam et al. 2003). Chemseddine and Moritz found that TiO_2 NPs with pure anatase form and with different shapes and sizes and with higher crystallinity can be obtained by polycondensation of titanium precursors with tetramethyl ammonium hydroxide (Chemseddine and Moritz 1999; Moritz et al. 1997). During the process, titanium precursor is mixed with base in the presence of a solvent and heated at 100 °C for 6 h. In order to improve crystallinity, TiO_2 NPs were heated again at 200 °C in an autoclave.

Sugimoto et al. studied the synthesis of TiO_2 NPs for distinctive shapes and sizes by changing process variables via sol-gel process. In the synthesis mechanism, a stock solution is prepared with TEOA (triethanol amine) and TTIP (titanium tetraisopropoxide) mixed in a ratio of 1:2. The pH of the stock solution was maintained with NaOH or $HClO_4$. The dilution of the stock solution was carried out by adding amines solutions into it. These amines are utilized as shape controllers and work as surfactants for TiO_2 NMs. They summarized the effect of pH in the adsorption of shape controller which further controls the growth rate of crystal lattice attributed to a crystal plane. Typical TEM images of the resulting solid product are presented in Fig. 8 (Sugimoto et al. 1997; Sugimoto et al. 2003a, b). El-Shafei et al. explained sol-gel synthesis of TiO_2 NPs for antimicrobial and flame-retardant cotton fabric by using chitosan phosphate and TTIP in the presence of poly carboxylic acid and sodium hypophosphite as a catalyst. The results explained that treated fabric showed excellent antimicrobial properties against *S. aureus* (*Staphylococcus aureus*), *E. coli* (*Escherichia coli*), *C. albicans* (*Candida albicans*) and *Aspergillus flavus* (El-Shafei et al. 2015). In another study, Roy et al. developed TiO_2 NPs by using citric acid and alpha dextrose and examined the effect of TiO_2 NPs on antimicrobial efficiency of different antibiotics. They used different concentrations of TiO_2 NPs to achieve the best output for antimicrobial activity. They used disk diffusion method in their study. They summarized that the antimicrobial resistance of methicillin-resistant *S. aureus* against various antibiotics is decreased with TiO_2 NPs and increased without TiO_2 NPs (Roy et al. 2010). Li et al. developed a crack free mesoporous

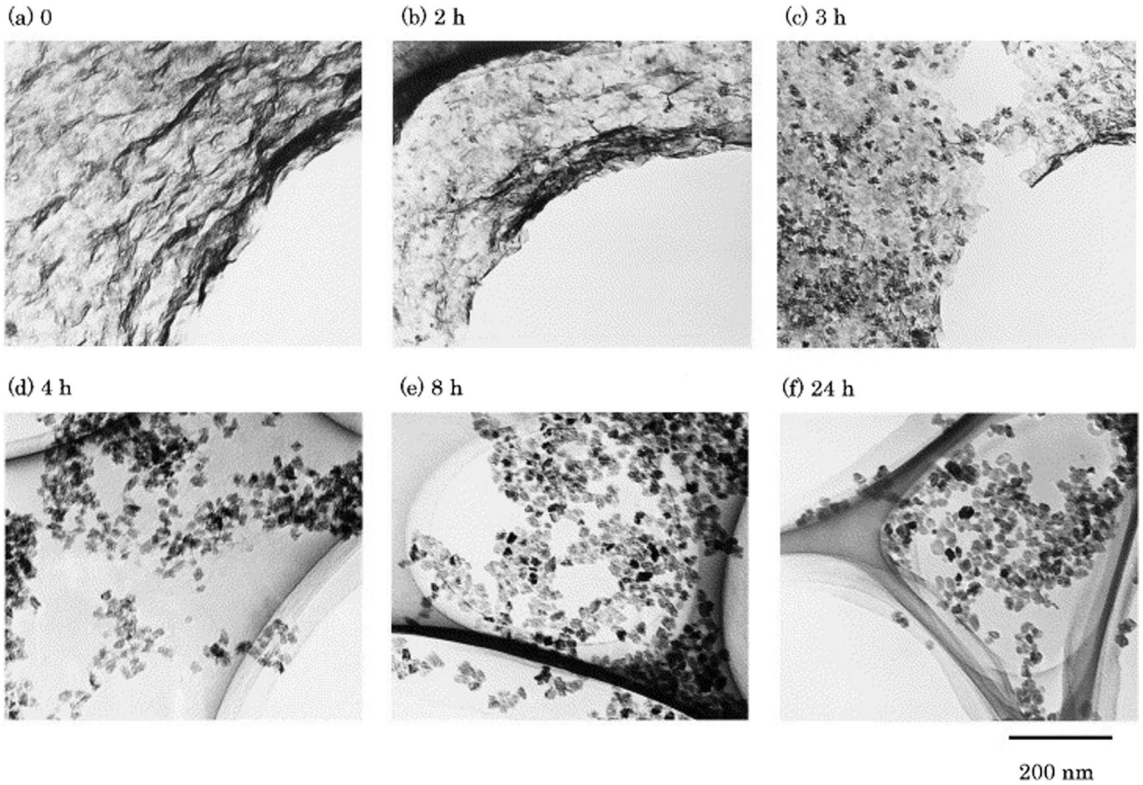

Fig. 8 **a**–**f** TEM micrographs of the solid product at different times (0 h to 24 h) during the second aging under the standard conditions. Reprinted with permission from Sugimoto et al. (2003a)). Copyright 2003, with permission from Elsevier

membrane with TiO_2 NPs by using a polymeric sol-gel method. They reported that developed crack free mesoporous membrane possesses high flux and deliver excellent separation performance. Moreover, the stiffness and toughness of the synthesized gel were significantly improved by adding TiO_2 NPs and the toughened gel was more capable of avoiding membrane cracking in early stages of sintering and during the drying process (Li et al. 2014).

Wang et al. utilized a sol-gel approach at room temperature to develop monodisperse spherical TiO_2 NPs modified with

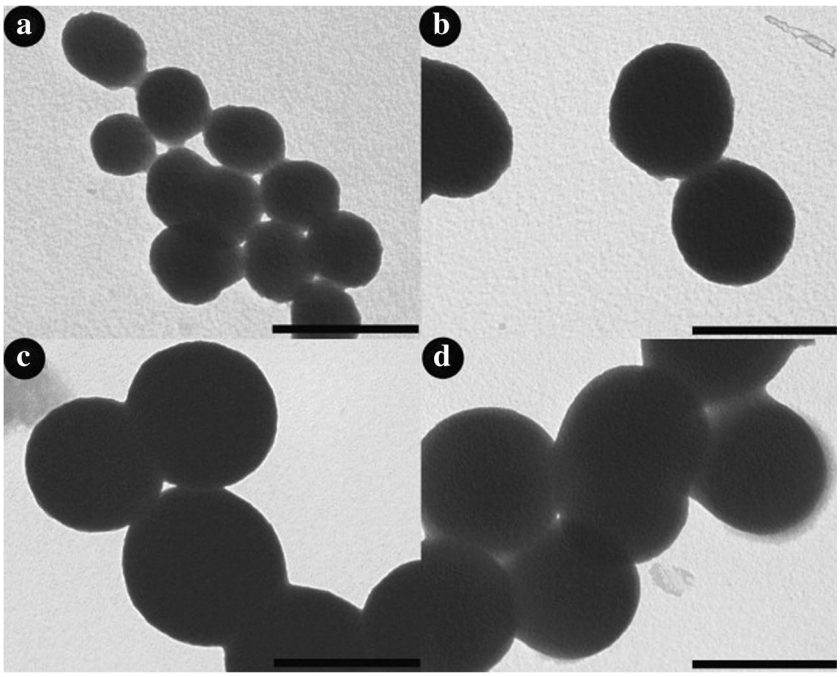

Fig. 9 TEM micrographs of TiO_2 particles synthesized with different acetone/water volume ratio. **a** 95/5, **b** 98/2, **c** 99/1, and **d** 99.5/0.5 using diethylene glycol. The scale bar is 500 nm. Reprinted with permission from Wang et al. (2014b)). Copyright 2014, with permission from Elsevier

EG (ethylene glycol). The photocatalytic performance of resulting photocatalyst was evaluated against MB (methylene blue) degradation under UV light irradiations. They summarized that the photocatalytic performance of the developed photocatalyst depends upon calcination and sample calcined at 600 °C exhibited excellent performance in dye degradation. TEM images of fabricated TiO_2 NPs are presented in Fig. 9 (Wang et al. 2014b). Uddin et al. established a low temperature sol-gel technique for the preparation of TiO_2 films on cellulosic fibers with enhanced photocatalytic properties. The photodegradation of heptane-extracted bitumen fraction and adsorbed MB was sustained with numerous impregnated photodegradation cycles. Interestingly, the surface of fiber was not changed upon light exposure. Moreover, the photoactive film was firmly attached with the fiber surface leading a retained photocatalytic performance even after 20 washing cycles (Uddin et al. 2007).

Jiu et al. produced single phase pure nanocrystals of anatase TiO_2 with average diameter 3–5 nm by using sol-gel process. TEM and XRD analysis confirmed pure anatase form of the resulting nanocrystalline TiO_2 (Jiu et al. 2007). Cai et al. synthesized highly porous TiO_2 microspheres by using cellulose nanofibril-based aerogel templates under sol-gel process. They reported that the developed TiO_2 microspheres had a super hydrophobic nature. Figure 10 represents the SEM images of nanofibril aerogels with TiO_2 microspheres (Cai et al. 2015). A sol-gel coupled with solvothermal process was utilized by Valencia et al. for developing highly photoactive nano-TiO_2 for photocatalytic applications. They stated that pure anatase phase was obtained at low temperature and short crystallization time by using 2-propanol as a solvent and tetraisopropyl orthotitanate as a precursor. The photodegradation of MO (methyl orange) showed the potential of synthesized nano-TiO_2 for their photocatalytic performance. SEM images of the developed nano-TiO_2 are described in Fig. 11 (Valencia et al. 2013). Mohammadi et al. reported that nanocrystalline TiO_2 powder with anatase form can be obtained by controlling the peptization and drying temperatures. The average size of the crystallite for the prepared powder was 4 nm after annealing (Mohammadi et al. 2008).

Mutuma et al. developed TiO_2 NPs from different mixtures of TiO_2 crystal polymorphs via low temperature sol-gel process. The samples were obtained by calcination at 200–800 °C. Anatase-rutile-brookite mixture was obtained at temperature > 600 °C while at 800 °C, anatase-rutile mixture was obtained under controlled pH. The photocatalytic activities of the developed photocatalysts in comparison with commercially available Degussa P25 photocatalyst was significantly higher indicating the smaller particle sizes and higher crystallinity which are required for heterogeneous photocatalysts. The XRD analysis of the developed samples at different pH is presented in Fig. 12 (Mutuma et al. 2015).

Chibac et al. described the preparation of hybrid photocross-linked nanocomposites incorporated with TiO_2 and silsesquioxane via sol-gel process combined with photopolymerization processes and photoinduced development of metal NPs in the polymer network. The results showed good photoreactivity of the monomer in photopolymerization reactions. The proposed method offers

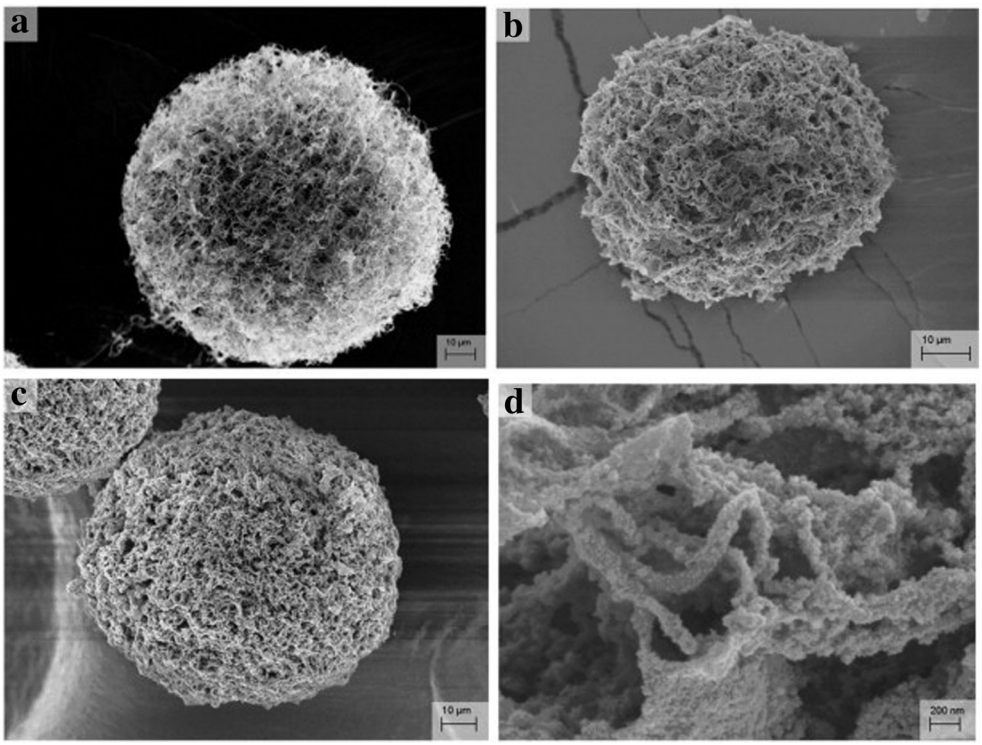

Fig. 10 SEM images of cellulose nanofibril aerogel microsphere and TiO_2 porous microspheres. **a** Cellulose nanofibril aerogel microsphere template. **b** TiO_2 porous microsphere prepared by the hydrolysis and polycondensation of titanium precursors in templates loading three times. **c** TiO_2 porous microsphere prepared by the hydrolysis and polycondensation of titanium precursors in templates loading seven times. **d** TiO_2 porous microsphere under higher magnification. Reprinted with permission from Cai et al. (2015)). Copyright 2015, with permission from Elsevier

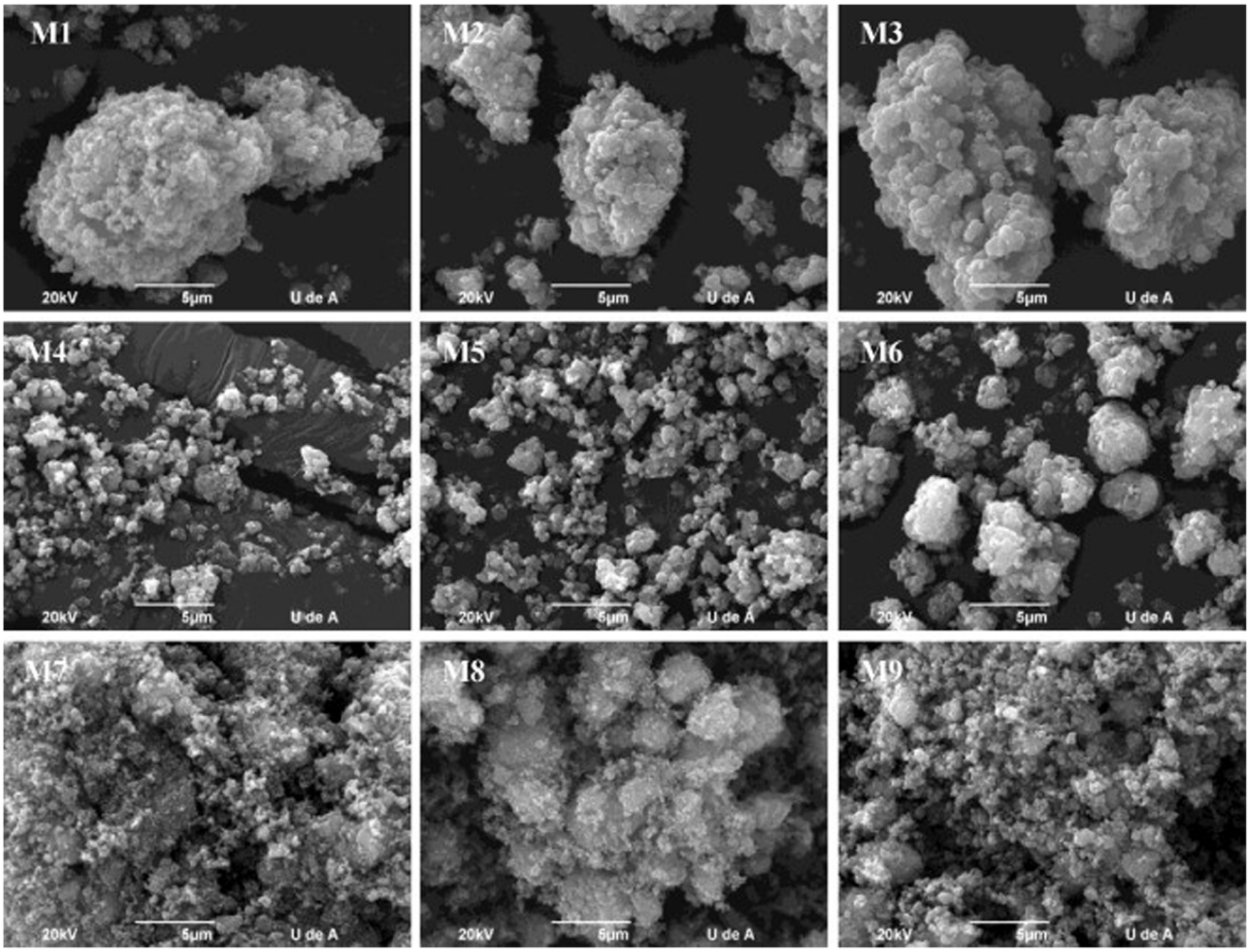

Fig. 11 SEM images of prepared TiO_2 samples. Reprinted with permission from Valencia et al. (2013)). Copyright 2013, with permission from Elsevier

a proper photocatalytic capability that recommends its usage in water purification applications (Chibac et al. 2015). Prasad et al. developed TiO_2 by using sol-gel process modified by ultrasound as a reaction aid with varying amplitude and power of ultrasonic energy. The best results were obtained by using 40% amplitude with input power of 751 kW m^{-3} for the synthesis of pure rutile form of nano-TiO_2. Moreover, the crystallinity was also very high under these conditions (Prasad et al. 2010). In another study, Kale and Meena synthesized TiO_2 NPs by sol-gel method and deposited on nylon fabric to investigate the antimicrobial properties. The durability of used process was evaluated after successive washing cycles indicating its effectiveness (Kale and Meena 2012). Wang et al. described the synthesis of TiO_2/diatomite composites by using a modified sol-gel process. Diatomite is a mineral utilized to develop these nanocomposites. The synthesized composites comprise a mixture of anatase and rutile. Photocatalytic performance and adsorption capacity of synthesized nanocomposites was assessed against photodegradation of RB (Rhodamine B) in UV irradiations. Photodegradation of RB followed pseudo-first-order kinetics (Wang et al. 2015a).

Qiu and Kalita synthesized nanocrystalline TiO_2 powder via simple sol-gel method. The synthesized powder was further calcined at 400 °C and had pure anatase form as confirmed by XRD study but rutile and anatase both phases were present at 600 °C with high phase content of rutile. A schematic illustration of developed nano-TiO_2 is presented in Fig. 13, while HRTEM micrograph of nano-TiO_2 is presented in Fig. 14 (Qiu and Kalita 2006). Velhal et al. described the synthesis of TiO_2 NPs by reacting butanol and HCl or H_2SO_4 with $TiCl_4$ (titanium tetrachloride) under a rapid sol-gel process. Amorphous and crystalline samples were obtained as confirmed by XRD analysis. The developed NPs were further utilized in antimicrobial applications and the results showed good antimicrobial efficiency than commercially available TiO_2 named Degussa P25 (Velhal et al. 2014). Caratto et al. utilized different methods to synthesize iron-doped TiO_2 NPs with different reagents ratios to estimate the effect of reagents on chemical and physical properties of Fe-doped TiO_2 NPs and on the photocatalytic activity. In a typical process, TTIP, 2-propanol, and iron chloride were used as titanium precursor, solvent, and dopant respectively (Caratto et al. 2016).

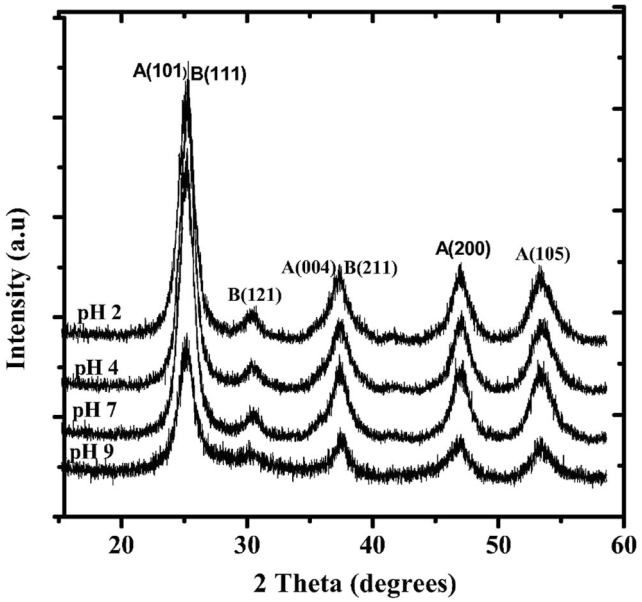

Fig. 12 XRD analysis of the synthesized TiO_2 samples at pH 2, 4, 7, and 9 and calcined at 200 °C. Reprinted with permission from Mutuma et al. (2015)). Copyright 2015, with permission from Elsevier

The formation of TiO_2 nanotubes doped with Fe was reported by He. The author studied the photocatalytic properties and operational parameters in dye degradation process. The author results explained that hybrid structures showed much higher surface area and excellent functional properties (He 2016). He and Tian prepared doped and undoped TiO_2 nanotubes under hydrothermal sol-gel method in aqueous NaOH solution. Their results showed that doping of Fe increased the photocatalytic performance of nanotubes (He and Tian 2016). In another study, He synthesized MoS_2/TiO_2 and MoS_2/Si-doped TiO_2 nanotubes that exhibit 1 T structure. The synthesized nanotubes showed much higher electrocatalytic and photocatalytic performance with higher interface-induced effect and higher light absorbance effect than normal nanotubes (He 2017a). In a different study, He and He used hydrothermal process for the fabrication of N-doped TiO_2 nanotubes with higher content of nitrogen, i.e., 25.7% that narrowed down the band gap which gives the extended absorption towards the visible and infrared regions (He and He 2011). He prepared ultrafine nanocrystalline Bi_2S_3 Fe-doped TiO_2 nanotubes with different approaches that provided good optical, structural, and photocatalytic properties (He 2017b). He et al. worked with transition metals that provide good catalytic performance for H_2 generation. They fabricated TiO_2 nanotubes in doped and undoped forms that showed excellent performance in photocatalytic H_2 evolution than other nanotubes (He et al. 2018).

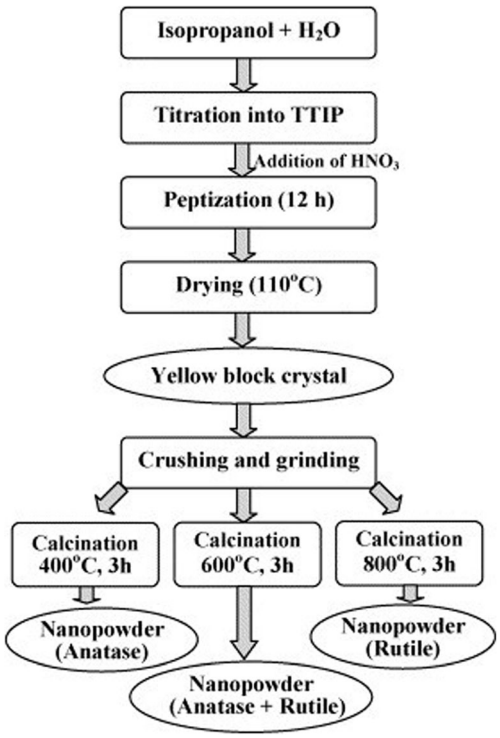

Fig. 13 Flow chart for the synthesis of nano-TiO_2 powders by sol-gel process. Reprinted with permission from Qiu and Kalita (2006). Copyright 2006, with permission from Elsevier

Hydrothermal synthesis

This method is conducted in autoclaves under controlled atmospheric conditions (pressure and temperature). The temperature raised above 100 °C and reaches to saturated vapor pressure. In ceramics industry, this technique is usually used for synthesis of small particles. Many researchers have utilized this method to prepare TiO_2 NPs (Andersson et al. 2002;

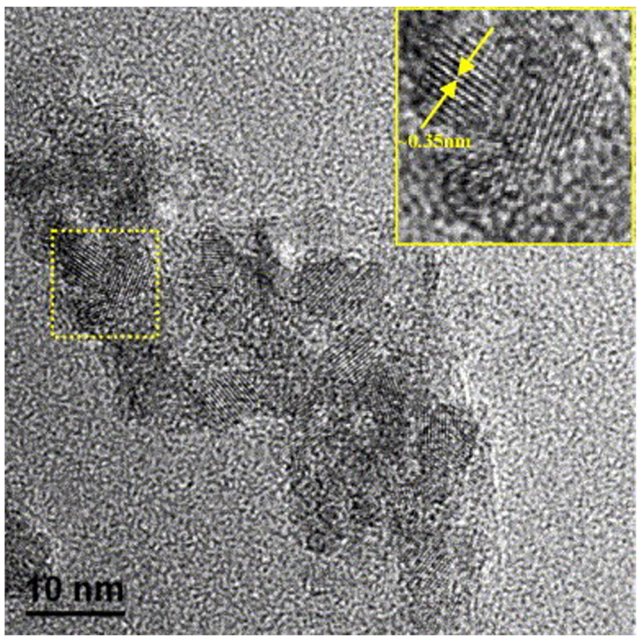

Fig. 14 HRTEM image of nano-TiO_2 powder prepared by sol-gel process and calcined at 400 °C. Reprinted with permission from Qiu and Kalita (2006). Copyright 2006, with permission from Elsevier

Chae et al. 2003; Cot et al. 1998; Yang et al. 2004b). Chae et al. prepared TiO_2 NPs by reacting TTIP in an acidic ethanol-water solution via hydrothermal method. In a typical approach, a dropwise addition of TTIP in a mixture of ethanol-water and reacted for 4 h at 240 °C. The synthesized TiO_2 NPs possessed the primary assembly of anatase. The size range of NPs was 7–25 nm which was controlled by adjusting the composition of the solvent and the concentration of precursor (Chae et al. 2003). Zhang and Gao synthesized TiO_2 nanorods by hydrothermal method. They reported that TiO_2 nanorods can be obtained by reacting titanium precursor with acid or inorganic salts at 333–423 K. TEM images of the synthesized TiO_2 nanorods by hydrothermal method are illustrated in Fig. 15 (Zhang and Gao 2003). Feng et al. reported an assembled TiO_2 nanorods films on glass wafer. They prepared these nanorods by reacting titanium trichloride with NaCl at 160 °C for 2 h via hydrothermal process (Feng et al. 2005).

Makwana et al. used the pilot plant scale CHFS (continuous hydrothermal flow synthesis) to control crystallite size and surface area of prepared nano-TiO_2. In a typical procedure, boric acid and titanium oxysulphate were mixed with KOH (potassium hydroxide) solution at room temperature under pressure 24.1 MPa. After that, this solution was mixed at 400 °C with superheated water in a closed mixer. Moreover, boric acid concentration was affected by pH of the solution which defines crystallite size. This increased the crystallite size of TiO_2. The photocatalytic activity of the synthesized nano-TiO_2 was estimated in water splitting system. The results revealed that mild acidic conditions used for the preparation of nano-TiO_2 yielded the highest photocatalytic performance. HRTEM micrographs of nano-TiO_2 synthesized by CHFS are presented in Fig. 16 (Makwana et al. 2016).

Kobayashi used water-soluble titanium complexes during a hydrothermal process to produce different polymorphs of TiO_2 by adding different additives to control the morphology of different structures. The developed polymorphs with controlled structures had excellent properties (Kobayashi 2016). Fan et al. synthesized mesoporous Ce-doped TiO_2 NPs with pure anatase form through one step hydrothermal process. They summarized that Ce doping reduced the crystallite size of TiO_2 NPs and the prepared samples showed highly significant photocatalytic performance than P25 and pure TiO_2

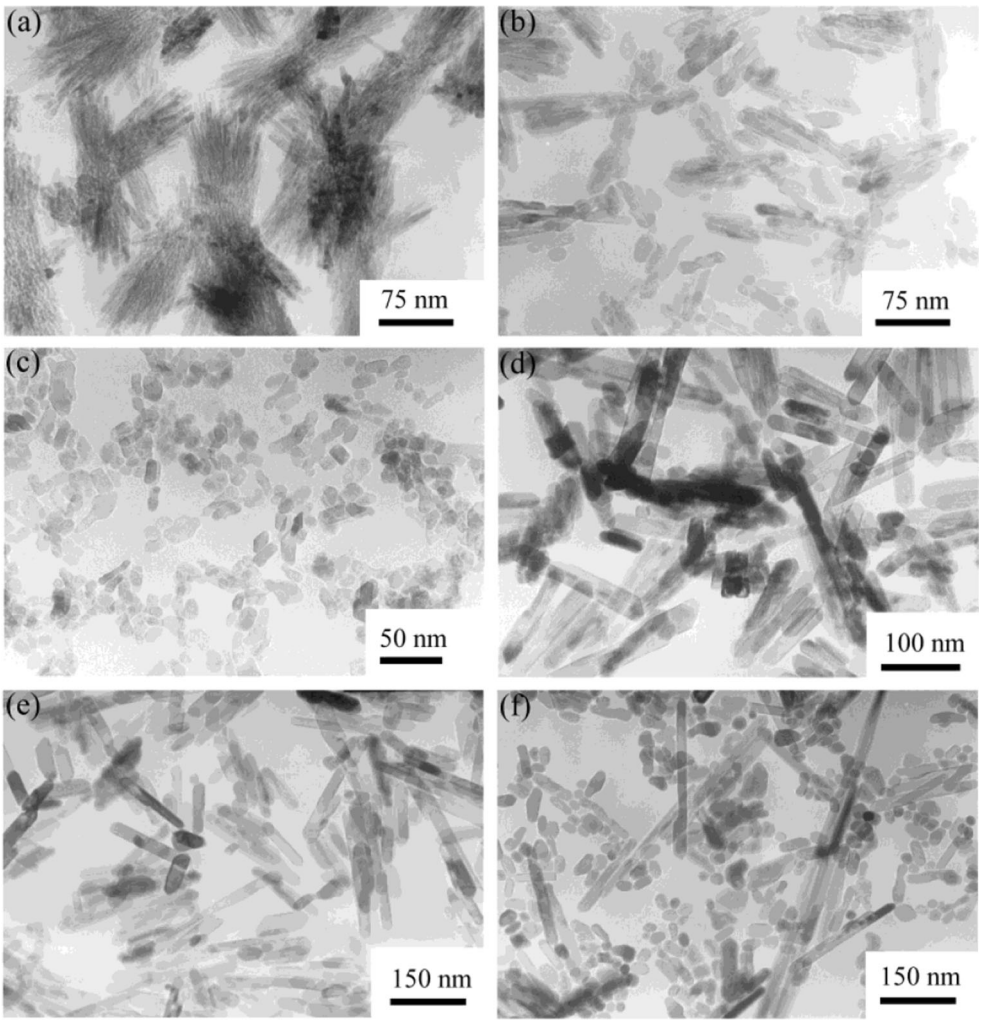

Fig. 15 TEM images of nano-TiO_2 prepared by the hydrothermal treatment of $TiCl_4$ solutions: **a** sample A, **b** sample C, **c** sample J, **d** sample K, **e** sample L, and **f** sample M. Reprinted with permission from Zhang and Gao (2003). Copyright 2003, with permission from American Chemical Society

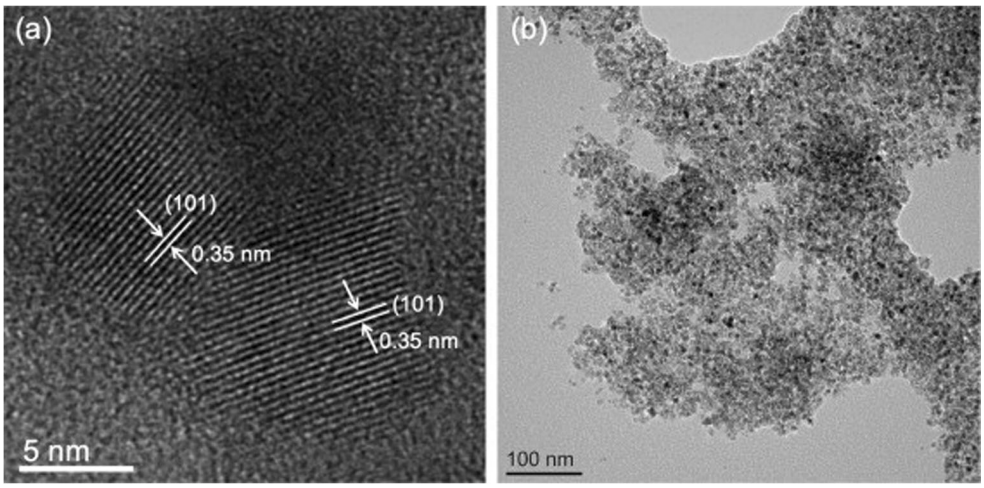

Fig. 16 HRTEM image of nano-TiO_2 synthesized by CHFS (**a**) with 1.5 mol% H_3BO_3 (**b**) with 10 mol% H_3BO_3. Reprinted with permission from Makwana et al. (2016)). Copyright 2016, with permission from Elsevier

against Rhodamine B dye degradation under UV light. This unique photocatalytic property of the synthesized samples enhanced generated charge carriers (electron-hole pairs) efficiency as well as more formation of ROS (Fan et al. 2016). Dong et al. developed a super hydrophilic film with TiO_2 nanorods on glass substrates by using hydrothermal process. They explained that TiO_2 nanorods in rutile phase with different diameter, orientation, and dispersing density were deposited on glass and FTO (fluorine-doped tin oxide) plates under the assistance of TiO_2/SiO_2 primary film. Typical TEM, SEM, and AFM images of the prepared TiO_2 NPs are presented in Fig. 17 (Dong et al. 2015). The ternary nanocomposites of PANI/C/TiN (polyaniline/carbon/titanium nitride) nanowire array were prepared by Xie et al. for flexible supercapacitor applications. These nanocomposites were used as electroactive electrode material in many devices. In a typical synthesis of these nanocomposites, titanium nitride nanowires array was formed by ammonia nitridation treatment under seed-assisted hydrothermal reaction. Then a sequentially carbon and polyaniline coatings were deposited on TiN nanowires surface. These PANI/C/TiN nanowires had an exceptional shell/shell/core architecture. These nanowires provide ion diffusion channel and electron transfer route among the neighboring nanowires. A schematic representation of synthesis process is illustrated in Fig. 18 (Xie et al. 2015).

Sarkar and Chattopadhyay prepared hierarchical TiO_2 nanobelts with controlled branches by varying the reaction time and temperature under hydrothermal conditions. These TiO_2 nanobelts were first synthesized in a Teflon autoclave which further assembled by branches via chemical bath deposition method. Photocatalytic activity of developed nanobelts was estimated against photocatalytic degradation of MO dye. The obtained results recommend the use of these nanobelts in hydrogen generation, water splitting, sensors, devices, and many other applications. FESEM and HRTEM micrographs of the synthesized samples are presented in Figs. 19 and 20 respectively (Sarkar and Chattopadhyay 2014). Li et at. reported a synthesis of anatase TiO_2 nanoflowers assembled on rutile nanobelts framework via simple hydrothermal process. These novel nanocomposites exhibited significant higher photocatalytic performance than pure TiO_2 nanobelts and Degussa P25 NPs against organic pollutants. The higher photocatalytic activity of these complex nanostructures increases photogenerated charge carriers transport. Moreover, these

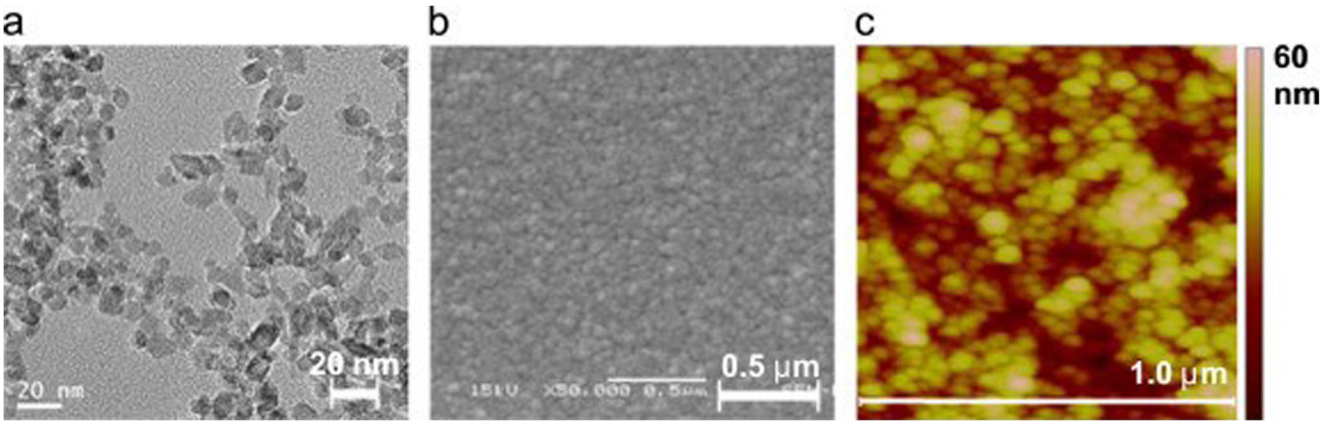

Fig. 17 Micrographs of TiO_2 NPs. **a** TEM, **b** SEM, and **c** AFM images of the film. Reprinted with the permission from Dong et al. (2015)). Copyright 2015, with permission from Elsevier

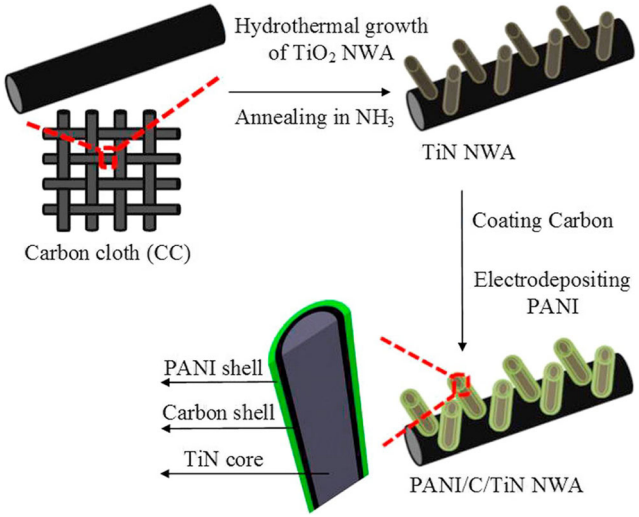

Fig. 18 The synthesis process for PANI/C/TiN NWA supported on CC substrate. Reprinted with the permission from Xie et al. (2015)). Copyright 2015, with permission from Elsevier

results showed that the prepared TiO_2 complex nanostructure possesses higher crystallinity and a double-crystal phase which enhance the photocatalytic performance for these nanostructures (Li et al. 2013). Wu et al. fabricated hierarchical nanowire arrays of anatase TiO_2 on FTO glass comprising long nanowire trunk associated with several short nanorod branches by utilizing hydrothermal process. The applications of these TiO_2 nanowire arrays showed 7.34% power conversion efficiency which was the highest reported value for TiO_2 nanowire photoelectrode. The higher photovoltaic performance was due to high surface area that adsorbed greater number of dye molecules with more light scattering capacity to increase light-harvesting efficiency (Wu et al. 2013). Zhang et al. described the synthesis of immobilized TiO_2 NPs on polyester fabric by using urea and titanium sulfate as reaction medium under hydrothermal conditions. The results confirmed the existence of pure anatase nanocrystals of TiO_2 on the surface of polyester fiber. Moreover, the anatase TiO_2 deposited fabric absorbed more UV light even after 30 washings. The hydrophilic nature was slightly increased and degradation of MO showed good photocatalytic performance of the resulting fabric (Zhang et al. 2012).

Yang et al. synthesized nanocrystalline anatase TiO_2 films under hydrothermal treatment by using TENOH (tetraethylammonium hydroxide)-peptized TiO_2 sols (as a novel stock precursor for synthesizing TiO_2 film) on silicon substrates with different solvents. They reported that highly homogeneous diluted TiO_2 sols were obtained by using acetone alone but the best combination of good wettability and high homogeneity was achieved by mixed solvents for silicon substrates (Yang et al. 2004a). In their previous study, Yang et al. prepared TiO_2 nanopowders through hydrothermal treatment of TiO_2 sols with different categories of TANOH (tetraalkylammonium hydroxides). The use of different peptizers enhances the particle growth. The morphology was significantly affected by changing concentrations of peptizers. They reported pure anatase form of TiO_2 with all peptizers as confirmed by TEM analysis and illustrated in Fig. 21 (Yang et al. 2001).

In another study, Yang et al. synthesized weakly flocculated anatase aqueous suspensions in an in situ manner from amorphous TiO_2 peptized with different amounts of TENOH by using hydrothermal process. The results revealed that the use of TENOH peptize the amorphous TiO_2 and stabilize the suspensions (Yang et al. 2003). Zhang et al. reported a successful anatase TiO_2 synthesis in single crystalline nanowires manners with diameter 30–45 nm by hydrothermal method from TiO_2 NPs. These nanowires exhibited photoluminescence property as emitted green-blue light. A typical SEM micrograph of these nanowires is presented in Fig. 22 (Zhang et al. 2002). Kalpagam and Kannadasan reported a hydrothermal synthesis of TiO_2 NPs for wastewater treatment. Their focus was on the optimization of autoclave time. For varying autoclave time, temperature was adjusted at 150 °C. The results confirmed the presence of pure anatase phase and more autoclave time provided more crystallinity to the resulting NPs and enhanced their photocatalytic activity (Kalpagam and Kannadasan 2014). Kolen'ko et al. described successful production of TiO_2 and ZrO_2 crystalline nanopowders from aqueous solutions of the corresponding hydroxides and their amorphous gels at high temperature under hydrothermal treatments. They investigated particles size, morphology, and phase configuration of formed powders as well as their variations in response to temperature, pressure, solution concentration, and process duration (Kolen'ko et al. 2003).

Hebeish et al. prepared TiO_2 nanowires from TiO_2 NPs under strong alkaline medium by hydrothermal method. Further, the doping the silver on nanowires and NP surfaces was successfully done by reduction of Ag^+ ions into Ag metal. Moreover, nanocomposites developed by these nanowires and Ag-doped nanowires showed high photocatalytic efficiency against MB degradation under direct sunlight. The prepared nanocomposites exhibited good performance against *S. aureus* and *E. coli* as well as fungi that recommends their use in medical and industrial applications (Hebeish et al. 2013).

Nawaz et al. worked on graphene oxide/TiO_2 aerogel and developed strong coupling among graphene oxide and TiO_2. They used a single-step hydrothermal method for their study. The photocatalytic activity of the prepared aerogel was investigated in the photodegradation of carbamazepine (Nawaz et al. 2017).

Sonochemical synthesis

Sonochemical approach has been utilized in the synthesis of various nanostructured materials including colloids, alloys, oxides, carbides, and high surface area transition metals.

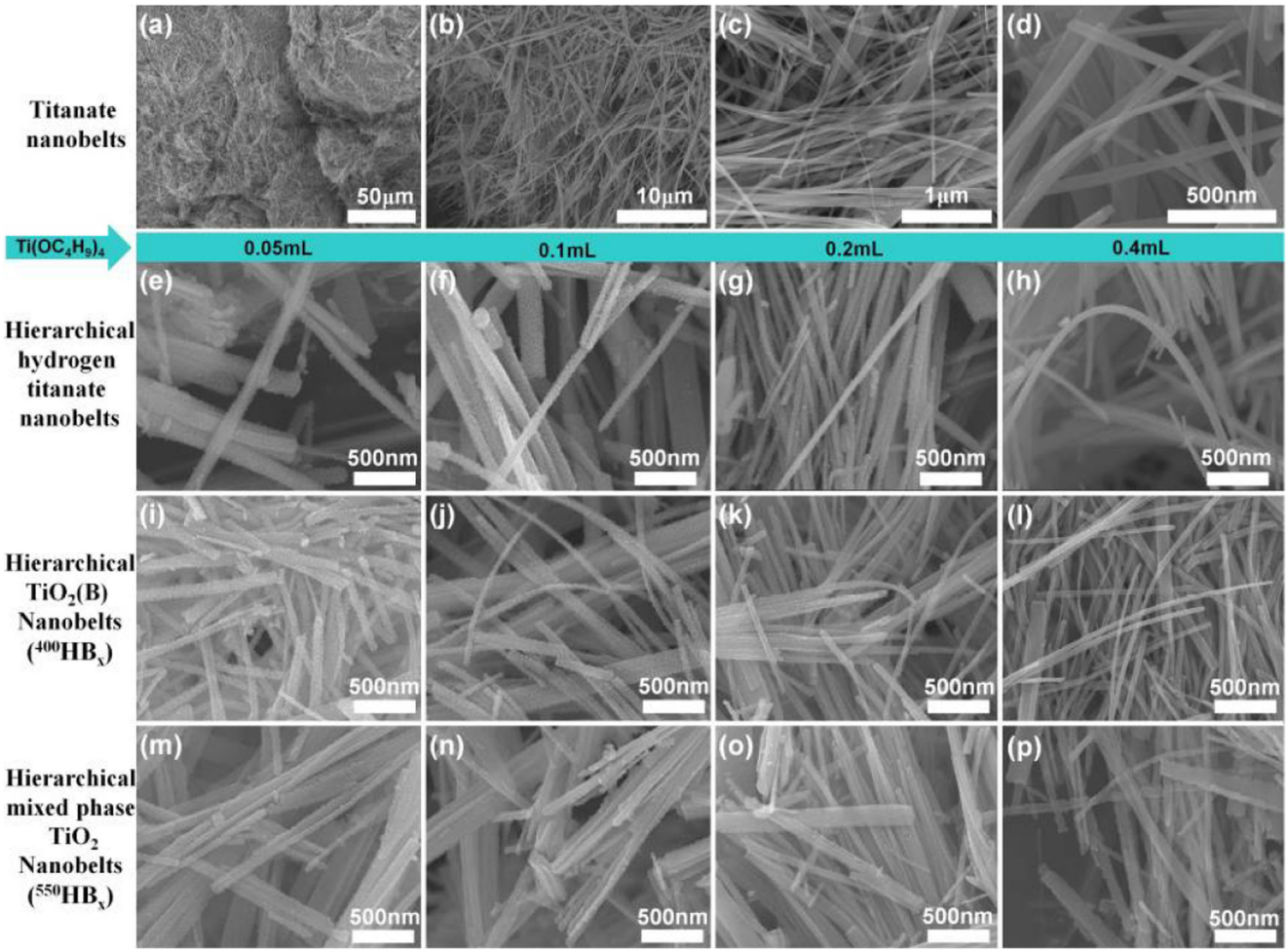

Fig. 19 FESEM micrographs of synthesized samples illustrate the progress of TiO_2 hierarchical structures under varying conditions. Bare TiO_2 nanobelts (**a**–**d**), hierarchical hydrogen titanate nanobelts (**e**–**h**), hierarchical TiO_2(B) nanobelts annealed at 400 °C (**i**–**l**), and hierarchical mixed phase TiO_2 nanobelts annealed at 550 °C (**m**–**p**). Reprinted with the permission from Sarkar and Chattopadhyay (2014). Copyright 2014, with permission from the American Chemical Society

Ultrasonic irradiations follow the principle of acoustic cavitation, i.e., rapid formation, growth, and collapse of unstable bubbles in liquids. These conditions raised local pressure and temperature up to 20 MPa and 5000 K with a cooling rate 10^{10} Ks^{-1} respectively (Suslick 1986).

Many researchers have applied this method to prepare numerous TiO_2 NMs. Jhuang and Cheng developed Ag/TiO_2 composite NPs in the presence of EG under alkaline conditions by using sonochemical method. They summarized that Ag^+ ions reduction in alkaline mixture of EG by ultrasonic irradiations is an autocatalytic reaction. The development of silver NPs on TiO_2 was observed through light absorption peaks of Ag NPs by UV-vis spectrophotometer. A schematic representation to the synthesized Ag/TiO_2 composite NPs is presented in Fig. 23 (Jhuang and Cheng 2016). Sadr and Montazer reported an in situ sonochemical synthesis of TiO_2 NPs on cotton by using TTIP as a titanium precursor. They summarized that at low temperature, TiO_2 NPs were successfully prepared and incorporated on cotton fabric. EDX and XRD analysis confirmed the existence of TiO_2 NPs with pure anatase phase on cotton. Moreover, the developed nanocomposites exhibited excellent self-cleaning, UV protection, and antimicrobial properties (Sadr and Montazer 2014). Arami et al. synthesized rutile TiO_2 NPs with average crystallite size 15 nm, diameter 20 nm, and surface area 78.88 m^2 g^{-1} through sonochemical method. They reported that aqueous NaOH broke Ti–O–Ti bonds in TiO_6 octahedra during initial reaction and then new octahedra were produced after ultrasonic irradiations (Arami et al. 2007).

Guo et al. described a novel sonochemical process for direct synthesis of anatase through hydrolysis of titanium alkoxide in ethanol and water at 90 °C for 3 h. They reported that the size and structure of NPs are dependent on reaction time, temperature and pH of the medium. Columnar shape of resulting NPs with average size 3–7 nm was found in TEM analysis (Guo et al. 2003). Behzadnia et al. reported TiO_2 NPs synthesis on wool fabric through hydrolysis of titanium alkoxide in acidic medium under a novel idea of in situ sonochemical synthesis at

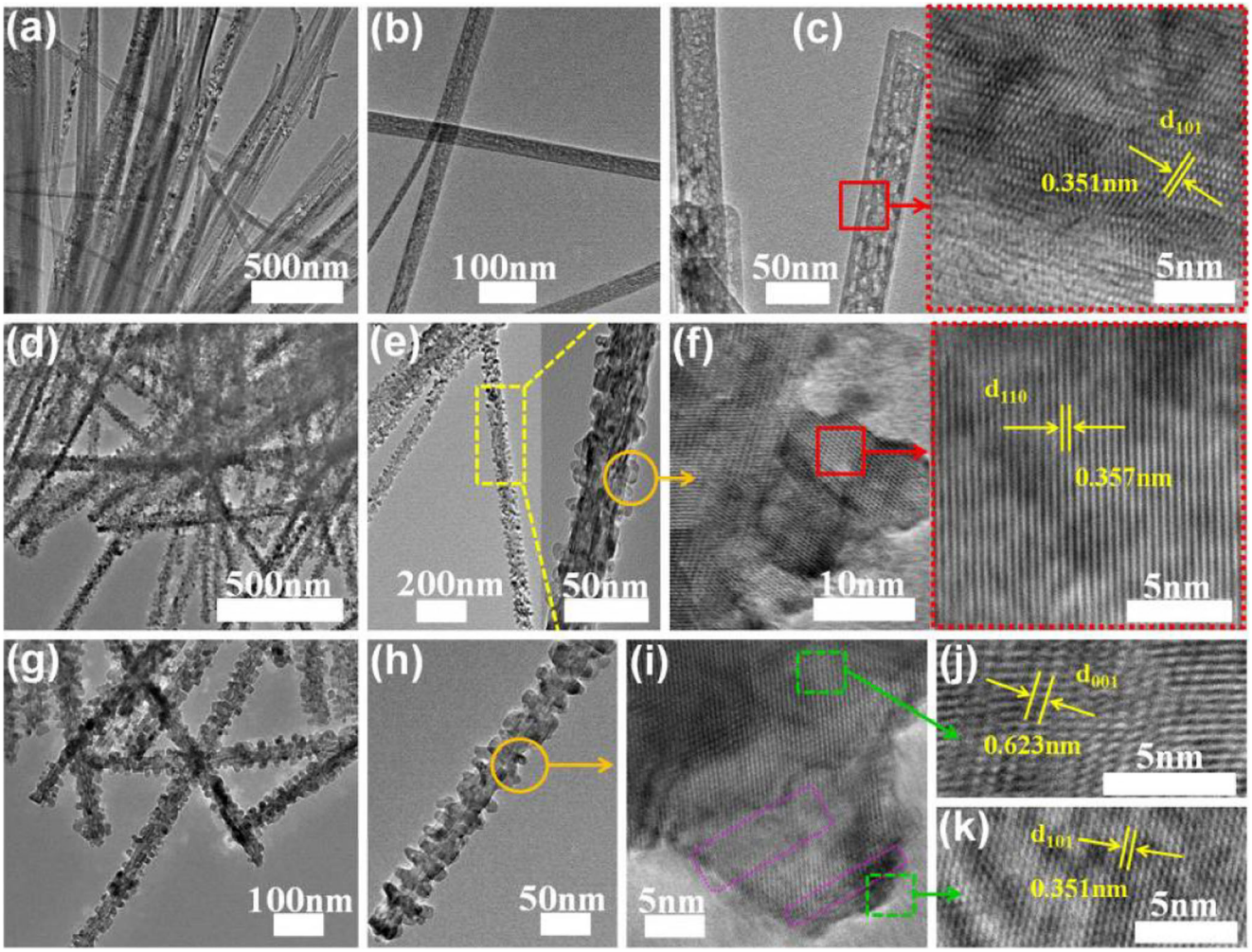

Fig. 20 HRTEM micrographs for synthesized TiO_2 nanostructures. Bare TiO_2 nanobelt (**a**–**c**), TiO_2(B) branched nanobelts (**d**–**f**), and mixed phase nanobelt with branch structures (**g**–**k**). Reprinted with the permission from Sarkar and Chattopadhyay (2014). Copyright 2014, with permission from the American Chemical Society

60–65 °C. The TiO_2 deposited wool fabrics possess significant self-cleaning and antimicrobial properties. This novel process had no negative effect on strength and cytotoxicity of TiO_2 coated wool fabric. In addition, more amount of titanium precursor results more photocatalytic performance of the sonotreated fabrics (Behzadnia et al. 2014b). In another study, Behzadnia et al. developed N-doped TiO_2 NPs on wool fabric by the hydrolysis of titanium isopropoxide in ammonia at low temperature by using in situ sonochemical method. The treated fabric had no negative influence on fibroblasts. The presence of TiO_2 NPs on wool was confirmed by EDX, elemental mapping and FESEM analysis. Moreover, the sonotreated wool fabric indicated some improved properties, e.g., tensile strength. Antimicrobial properties of the developed nanocomposites were evaluated against *S. aureus* and *E. coli* and good results were obtained (Behzadnia et al. 2014a). Blesic et al. prepared TiO_2 nanofilms by using TiO_2 NPs through ultrasonic spray pyrolysis. The appearance of the developed films revealed with rutile phase of TiO_2 as confirmed by XRD analysis. They concluded that morphology of the prepared films solely depends on temperature. In addition, ultrasonic spray pyrolysis provides an easy way to preparer a film with a porous structure or a compact smooth structure (Blešić et al. 2002). Meskin et al. developed different metal oxides nanopowders by ultrasonic assisted hydrothermal method using precipitated amorphous hydroxides as precursors (Meskin et al. 2006). Gedanken provided a detail review on the fabrication of NMs by using sonochemical method. The major focus of his work was on the synthesis of one-dimensional NMs, e.g., nanowires, nanorods, nanobelts, and nanotubes (Gedanken 2004). In our previous investigation, we utilized ultrasonic acoustic method to synthesize TiO_2 NPs with anatase form and average particle size 4 nm. We also developed a mathematical model based on interaction between individual factors and related responses. A comparative analysis of RNP (resulting nanoparticles) with P25 recommends them a strong candidate for photocatalytic industrial applications. The results of SEM analysis are presented in Fig. 24 (Noman et al. 2018b).

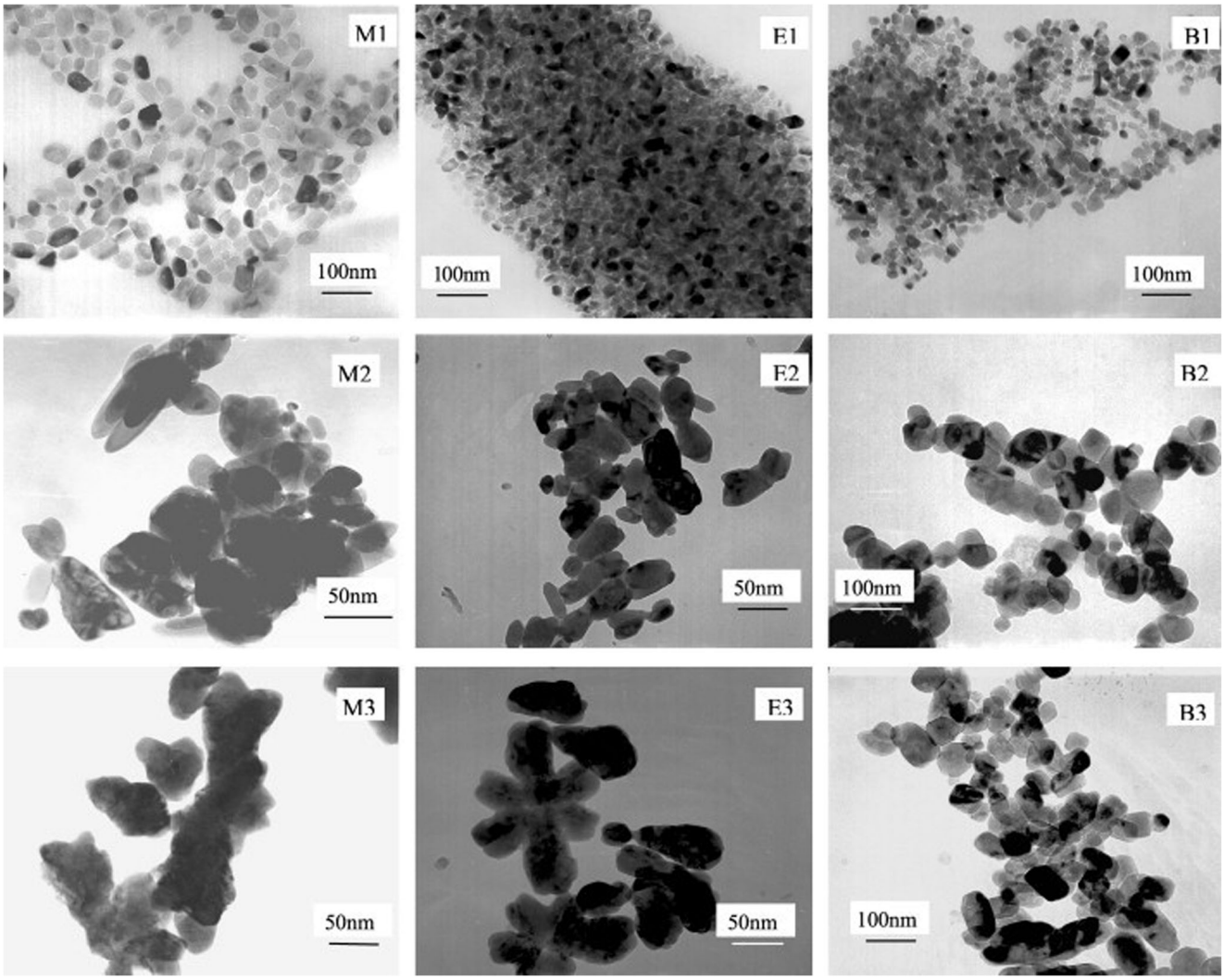

Fig. 21 TEM micrographs of the synthesized TiO_2 NPs. Tetramethylammonium hydroxides TMNOH/Ti ratio is taken as 0.25, 0.5, and 1.0 in samples M1 to M3. Tetraethylammonium hydroxides TENOH/Ti ratio is taken as 0.25, 0.5, and 1.0 in samples E1 to E3. Tetrabutylammonium hydroxides TBNOH/Ti ratio is taken as 0.25, 0.5, and 1.0 in samples B1 to B3 respectively. Reprinted with permission Yang et al. (2001)). Copyright 2001, with permission from Elsevier

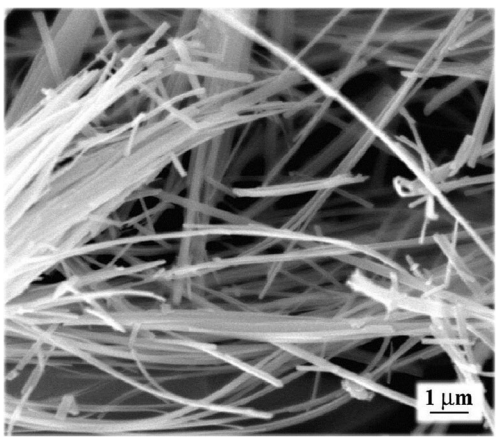

Fig. 22 SEM micrograph of TiO_2 nanowires. Reprinted with permission from Zhang et al. (2002)). Copyright 2002, with permission from Elsevier

Xue et al. described a novel ultrasound-assisted precipitation synthesis of AgI/TiO_2 nanocomposites with enhanced light absorption intensity and antimicrobial activity. AgI NPs coupling extended the photoresponse of the AgI/TiO_2 nanocomposites till visible range. The photocatalytic results revealed that $O_2^{\cdot-}$ (superoxide anion) and h^+ (holes) are the key constituents for the photodegradation of MO (Xue et al. 2015).

Wei et al. synthesized TiO_2 in aerogel form under ultrasonic assisted sol-gel technique that provides high surface area and special photocatalytic properties without annealing. Stannous chloride was used as a dopant in this study (Wei et al. 2018).

Miscellaneous methods

Fathy et al. reported a polyol-mediated solvothermal process for large-scale preparation of anatase TiO_2 with different

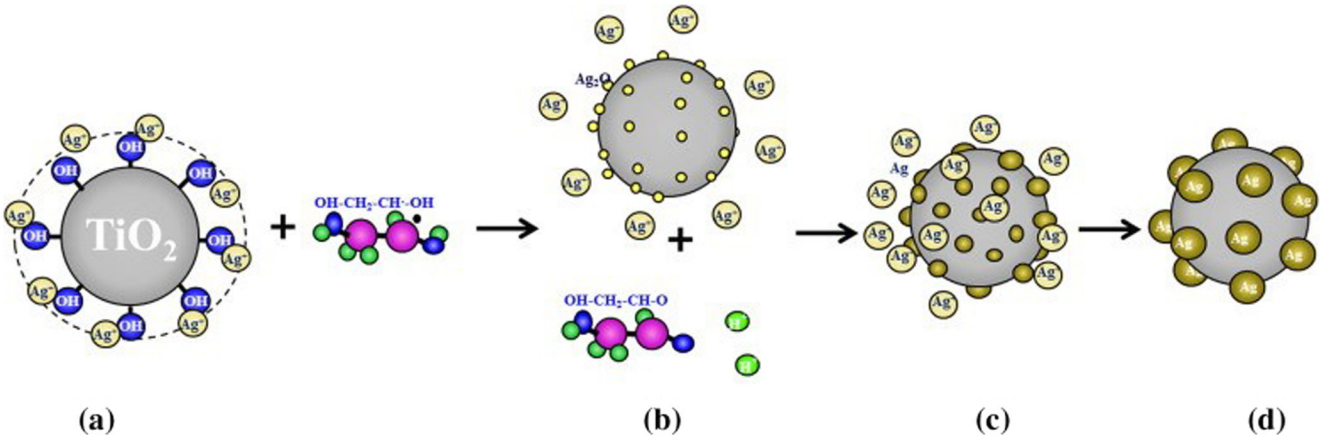

Fig. 23 The schematic representation of synthesized Ag/TiO_2 NPs: (a) Ag^+ ions attracted towards the OH group of TiO_2 and $OHCH_2CHOH$ free radical. (b) Crystal nucleus Ag_2O formed on TiO_2 and by products of H^+ ions and acetaldehyde. (c) Reduction of Ag^+ ions on crystal nucleus. (d) Ag NPs growth on TiO_2 in the sonochemical process. Reprinted with permission from Jhuang and Cheng (2016). Copyright 2016, with permission from Elsevier

morphologies (nanorods and NPs) by using TTIP as a precursor and EG as a surfactant. Calcination process had a prodigious influence on anatase nanorods production. Higher temperature provides higher phase stability of TiO_2 (Fathy et al. 2016). Yeung and Lam used an easy chemical vapor deposition method for the hydrolysis of $TiCl_4$ at 130–250 °C to produce TiO_2 films. The increased deposition temperature increases the refractive index of the developed films from 2.1 to 2.4 indicating the use of these films in antireflection coating for n-type semiconductors (Yeung and Lam 1983). Zhang et al. reported a rapid microwave-assisted method for synthesis of anatase TiO_2 nanocrystals with tuneable percentage of reactive exposed [001] facets. Photocatalytic performance was estimated through photodegradation of brilliant red X3B dye and photoluminescence of coumarin which is used as a probe molecule. These results revealed that surface chemistry and crystal planes perform an important role on photocatalytic performance of nanocrystals (Zheng et al. 2012). Hossain et al. described a steam-assisted process for large scale production of mesoporous uniform TiO_2 with pure anatase form. The photocatalytic performance of uniformly ordered anatase against MB and 4-chlorophenol decompositions were significantly higher to randomly mesoporous anatase and anatase NPs, indicating a solid reason to synthesize anatase in uniform mesoporous forms. A schematic representation of the three common forms of anatase TiO_2 is illustrated in Fig. 25 (Hossain et al. 2015). Wang et al. used a facile water-assisted technique for fabrication of anatase TiO_2 nanocrystals at low temperature with average size 2–4 nm. In a typical process, H_2O was used as a key reagent for fast crystallization of anatase formation under mild conditions while EG controls the rate of hydrolysis and condensation of titanium isopropoxide. The resulting anatase nanocrystals exhibited a quick response to oxygen under UV light illumination at room

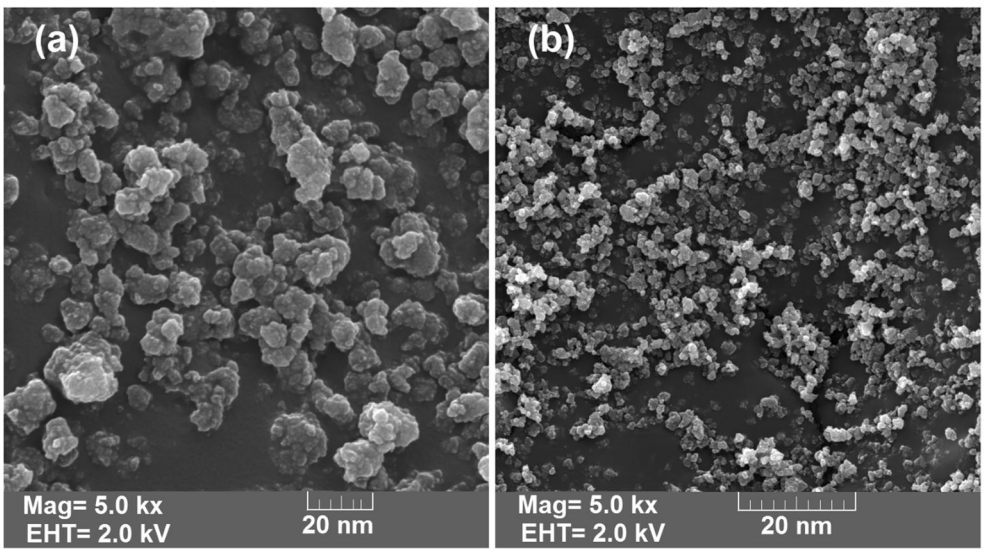

Fig. 24 SEM analysis. **a** P25 and **b** RNP with optimal conditions TTIP 10 mL, EG 4 mL, Sonication time 1 h. Reprinted with permission from Noman et al. (2018b)). Copyright 2017, with permission from Elsevier

temperature (Wang et al. 2008b). Dominguez et al. investigated the effect of microwave irradiations on stabilization and luminescent properties of TiO_2 and samarium-doped TiO_2 nanocrystals. In a typical study, benzyl alcohol was utilized as a solvent while annealing temperature range was 200–1000 °C. The results revealed that microwave irradiations allowed successful embedding of Sm^{+3} ions in crystal lattice of TiO_2 which distorted TiO_6 octahedron to replace Ti^{+4} ions (Dominguez et al. 2016). Zabova et al. demonstrated the synthesis of TiO_2 and V/TiO_2 nanocrystalline layers by utilizing microwave-assisted drying and calcination methods. The functional and photocatalytic properties of the nanocrystalline TiO_2 and V/TiO_2 thin layers were compared with conventional thin layers and quantified by the degradation rate of RB (Žabová et al. 2009).

Zhou et al. used an evaporation induced self-assembly process to synthesize thermally stable and highly mesoporous anatase TiO_2 having higher crystallinity attributed to encircling EN (ethylenediamine) protectors for sustaining mesoporous framework of TiO_2 primary particles. The results revealed that the developed samples exhibit higher photocatalytic performance than P25 for photodegradation of 2,4-dichlorophenol (Zhou et al. 2011). Teoh et al. introduced a facile one-step synthesis of TiO_2 and TiO_2/Pt NPs by FSP (flame spray pyrolysis). The resulted powders mostly composed of anatase TiO_2 with specific surface area and controlled crystallite size. The photocatalytic mineralization of sucrose showed that NPs synthesized by FSP follow a fast and different reductive pathway than Degussa P25 (Teoh et al. 2005). In another study, Teoh et al. synthesized Fe-doped TiO_2 with enhanced light activity through a direct FSP process for the photomineralization of oxalic acid. The results revealed that the rate of oxalic acid photomineralization under visible light irradiations by Fe-doped TiO_2 was 6.4 times higher than Degussa P25 and similarly prepared bare TiO_2. The minimal loss of Fe from TiO_2 surface after each run showed that Fe-TiO_2 photocatalyst was stable and reusable. Moreover, the UV-vis spectrum was unchanged after repeated photocatalytic runs. Typical TEM images of FSP-made NPs are presented in Fig. 26 (Teoh et al. 2007). Kadam et al. described a microwave-assisted technique to synthesize N-doped nano-TiO_2 with average size 10 nm. The developed NPs were thermally stable as confirmed by TGA-DTA (thermogravimetric-differential thermal analysis). A photodegradation of malathion showed that photodegraded products were less toxic than malathion as confirmed by cytotoxicological studies (Kadam et al. 2014).

Applications of nano-TiO_2

The most promising applications of nano-TiO_2 are photocatalytic and photovoltaic applications. The band gap of nano-TiO_2 is usually larger than 3.0 eV. The optical properties of nano-TiO_2 enables it a good choice for UV protecting applications.

Photocatalytic applications

TiO_2 is an environmentally benign and efficient material and extensively used in the photodegradation of numerous organic pollutants. Fujishima et al. described the mechanism of photocatalysis on surface of TiO_2 and discussed its practical interest in water purification, self-cleaning, self-sterilizing surfaces, and light-assisted H_2 production (Fujishima et al. 2008). Xiao et al. applied an inorganic TiO_2/Al_2O_3 nanolayers onto dyed blend of polyamide/aramid fabric by atomic layer deposition process to develop multifunctional fabrics that exhibit resistance to UV light. The successful deposition of TiO_2, Al_2O_3, and TiO_2/Al_2O_3 nanolayers on the surface of fiber was confirmed by EDX. The nanolayer-coated fabric showed excellent UV-resistant properties under high-intensity UV light (Xiao et al. 2015). Gaminian and Montazer investigated the self-cleaning of Cu_2O/TiO_2 on polyester fabric for automotive and upholstery applications. The results confirmed that the developed fabric displayed significant photocatalytic efficiency during the photodegradation of MB for both washed and unwashed samples. Moreover, the alkaline hydrolysis produces EG which acts as reducing agent for synthesis of

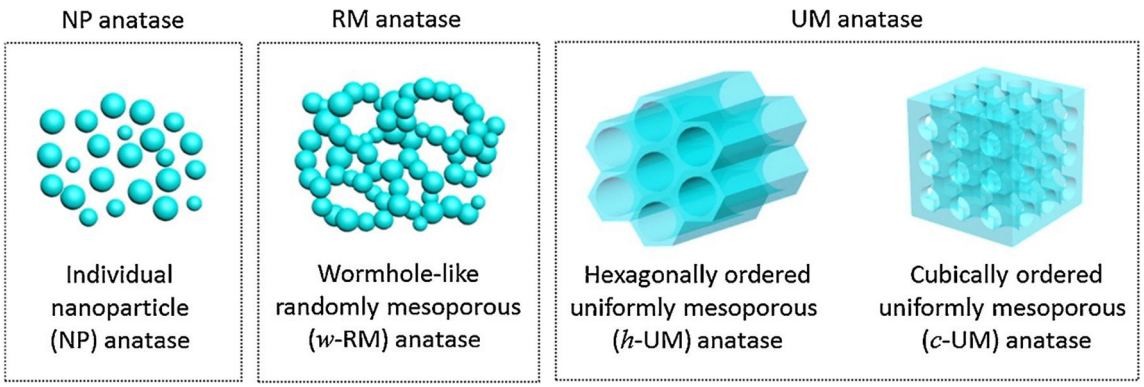

Fig. 25 The different forms of anatase TiO_2. Reprinted with permission from Hossain et al. (2015)). Copyright 2015, with permission from Elsevier

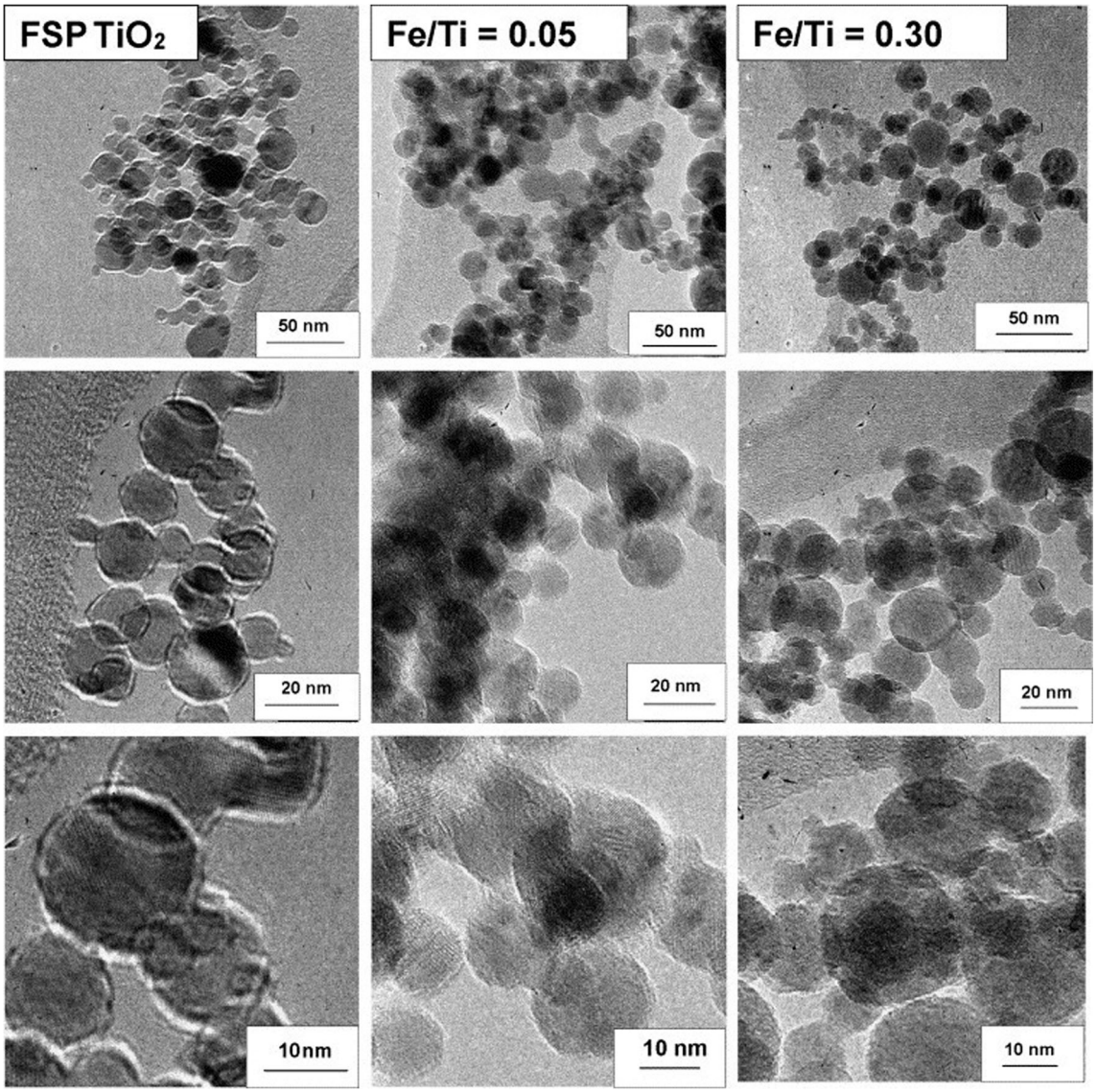

Fig. 26 TEM images. **a** TiO_2, **b** Fe/Ti = 0.05, and **c** Fe/Ti = 0.30 at different magnifications. Reprinted with permission from Teoh et al. (2007)). Copyright 2007, with permission from Elsevier

Cu NPs (Gaminian and Montazer 2015). Harifi and Montazer prepared iron-doped Ag/TiO_2 nanocomposites by a facile photodeposition/wet impregnation process for photocatalytic applications under UV-vis light irradiations. Photocatalytic efficiency of developed photocatalyst was estimated by photodegradation of MB under different light irradiations. The Fe^{3+} doping on TiO_2 structure and deposition of Ag NPs on TiO_2 surface were confirmed by XPS analysis. Ag and Fe^{3+} synergistically enhanced the photocatalytic performance of TiO_2 for photodegradation of MB under both UV and visible light regions. The proposed photocatalytic mechanism of Fe^{3+}:Ag/TiO_2 is described in Fig. 27 (Harifi and Montazer 2014).

Ghanem et al. described photocatalytic performance of hyperbranched PET/TiO_2 nanocomposites. In a typical process, first TiO_2 nanowires were synthesized in alkaline medium from TiO_2 NPs by hydrothermal method which further hyperbranched with polyester by polycondensation. The results summarized that the developed nanocomposites have extensively higher photocatalytic performance than the pure TiO_2 nanowires and degradation time was also reduced to great extent (Ghanem et al. 2014). Arain et al. studied antimicrobial efficiency of cotton fabric treated with chitosan/AgCl–TiO_2 colloid. In their study, they used diverse blend ratios of chitosan and AgCl–TiO_2 colloid to obtain maximum antimicrobial efficiency against microorganisms. The results revealed that the AgCl–TiO_2 colloid with chitosan provides much better antimicrobial properties to cotton fabric than the fabric treated without chitosan (Arain et al. 2013). Senic et al. produced smart textiles modified with TiO_2 NPs for self-decontaminating properties. They summarized the results by producing TiO_2 NPs at low temperature with different

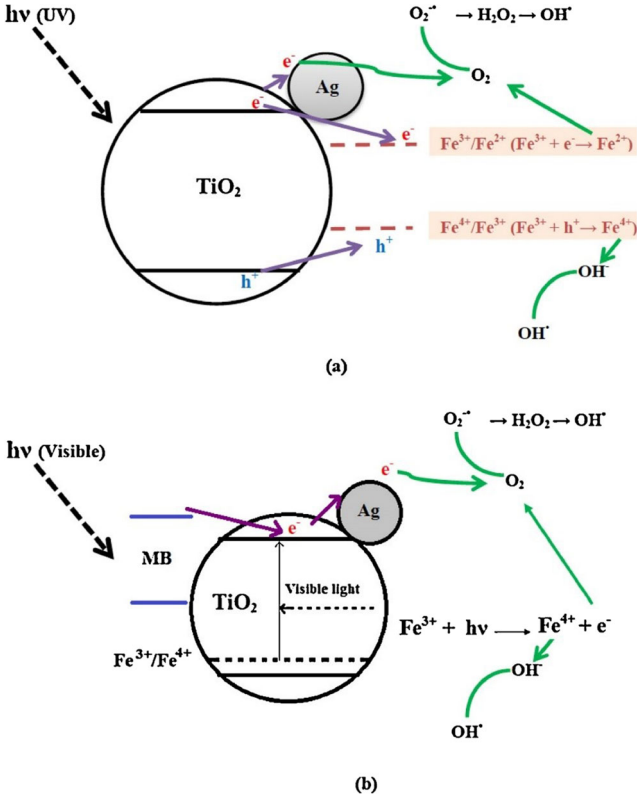

Fig. 27 The photocatalytic mechanism of $Fe^{3+}Ag/TiO_2$ photocatalyst under **a** UV light and **b** visible light irradiations. Reprinted with permission from Harifi and Montazer (2014). Copyright 2014, with permission from Elsevier

methods and then incorporate them on different textile substrates by different methods (Senić et al. 2011). Gupta et al. applied TiO_2 and ZnO NPs on cotton fabric by using low amount of binder and studied the functional properties of the finished fabric. These results revealed that TiO_2-coated cotton fabric exhibited significant self-cleaning efficiency on light exposure which could be improved by adding more amount of TiO_2 NPs (Gupta et al. 2007).

Wang et al. worked on surface modification of TiO_2 NPs to increase photocatalytic performance. They synthesized novel metal hydroxide/TiO_2 NPs by a simple wet precipitation route at low temperature and photocatalytic ability of synthesized nanocomposites was estimated against photodegradation of MO which was considered as an organic pollutant. The results explained that photocatalytic performance of modified TiO_2 was five times higher than the neat TiO_2 without modification (Wang et al. 2008a). Wiener et al. deposited TiO_2 NPs on the surface of glass fabric by a novel laser light irradiations method. The morphology of the treated fabric was evaluated by SEM, XRF, and EDX spectroscopies. The results showed that TiO_2 NPs deposited glass fabric showed a continuous decreasing trend in concentration of orange II dye under UV light irradiations which confirmed a promising photocatalytic activity of the TiO_2 NP-treated glass fabric (Wiener et al. 2013). Montazer et al. investigated the antimicrobial and antifelting properties of wool fabric treated with nano-TiO_2. In a typical study, fabric shrinkage after washing was estimated to study the antifelting properties while antimicrobial activities were evaluated against microorganisms. They used BTCA (butane tetracarboxylic acid) and CA (citric acid) as cross-linking agents to link TiO_2 NPs on the wool surface (Montazer et al. 2011b). Karahaliloglu et al. developed TiO_2/PP nanocomposites by melt electrospinning process as a photocatalyzer for dyeing wastewater decolorization. SEM results confirmed the uniform distribution of TiO_2 NPs on PP. Photocatalytic performance of developed nanocomposites was investigated against MO and the results revealed that TiO_2 NP-loaded GA (glutaraldehyde)-treated samples showed better photocatalytic properties and can be used as photocatalytic filter to decolorization of wastewater (Karahaliloglu et al. 2014). Qi et al. prepared a transparent thin layer of TiO_2 NPs on cotton fabric by using dip-pad-dry-cure process and investigated photocatalytic self-cleaning properties of developed cotton textiles. The results revealed that TiO_2-coated cotton exhibited excellent photocatalytic performance against coffee stains and red wine and colorant decomposition under UV light irradiations and significant antimicrobial performance was observed against *S. aureus* in comparison with untreated cotton (Qi et al. 2006). Behzadnia et al. reported a direct sonochemical synthesis of TiO_2 NPs on wool fabric by using titanium butoxide or titanium isopropoxide as titanium source to investigate functional properties of wool fabric. The results revealed that wool fabric with TiO_2 NPs exhibited significant antimicrobial and self-cleaning properties by degrading MB stains under sunlight irradiation (Behzadnia et al. 2014b). Wu et al. prepared self-cleaning fabrics by modifying cotton fabric with TiO_2 NPs at low temperature under an aqueous sol process. Pure anatase nanocrystals with 3–5 nm in size were successfully obtained by this approach as confirmed by HRTEM and XRD analysis. The results showed that the prepared cotton-TiO_2 nanocomposites possessed significant self-cleaning properties. The photocatalytic degradation of dyes and antimicrobial performance of the treated fabrics were sustained upon several numbers of reused cycles (Wu et al. 2009). Perelshtein et al. deposited TiO_2 NPs on cotton fabric by using a simple one-step ultrasonic irradiation process and investigated the antimicrobial properties of the developed cotton-TiO_2 nanocomposites against microorganisms. The antimicrobial results showed that developed nanocomposites had a significant effect against *S. aureus* bacteria (Perelshtein et al. 2012). In our previous study, we developed an in situ deposition of TiO_2 NPs on cotton fabric by ultrasonic acoustic method by using $TiCl_4$ and isopropanol as reactants and investigated the functional properties of the developed nanocomposites. The results of self-cleaning, antimicrobial efficiency, and UPF (ultraviolet protection factor) showed that the developed nanocomposites have highly photocatalytic activities. In addition, the washing durability results showed a strong

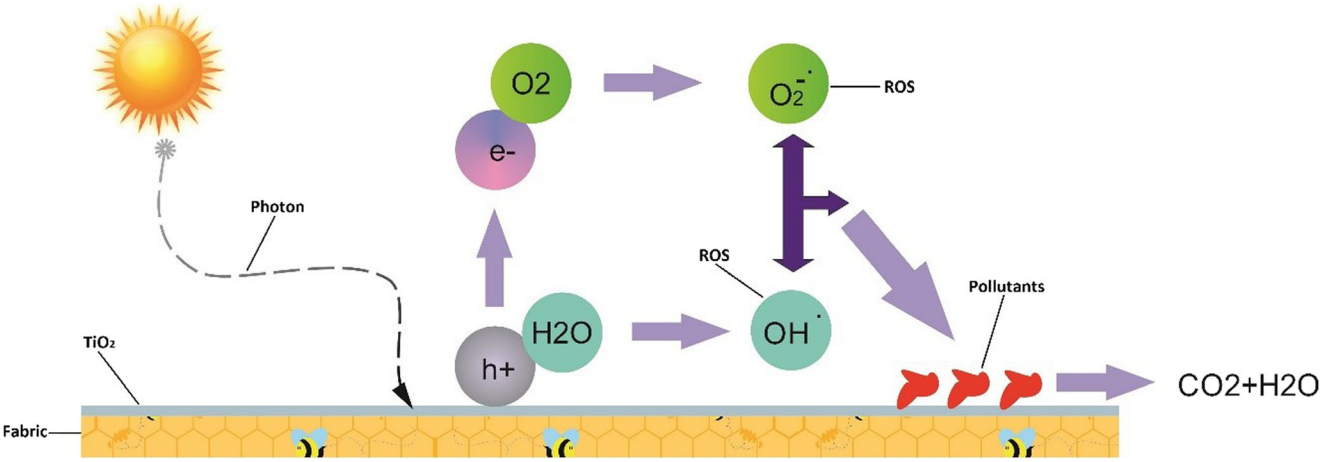

Fig. 28 Photocatalytic process on the surface of CT nanocomposites. Reprinted with permission from Noman et al. (2018c)). Copyright 2018, with permission from Elsevier

attachment of TiO_2 NPs with cotton surface. The mechanism of photocatalysis on surface of TiO_2 deposited cotton fabric is presented in Fig. 28 (Noman et al. 2018c).

Zhou et al. investigated photocatalytic activity of iron-doped mesoporous TiO_2 NPs prepared by sol-gel process against acetone. Their results explained that photocatalytic oxidation of acetone in air was significantly higher for iron-doped TiO_2 NPs as compared to bare TiO_2 and P25. Moreover, the doping of Fe in the mesoporous TiO_2 powders reduces recombination rate of charge carriers during heterogeneous photocatalytic reaction (Zhou et al. 2005). El-Roz et al. prepared luffa/TiO_2 nanocomposites from the hydrolysis of TiO_2 precursor for photocatalytic applications. The photocatalytic performances of the developed nanocomposites were investigated against methanol. The results showed a good stability of luffa/TiO_2 nanocomposites with enhanced photocatalytic performance under UV light irradiations, which provided a new class of green photocatalysts for photodegradation of organic pollutants (El-Roz et al. 2013). Doakhan et al. investigated the effect of TiO_2/sericin nanocomposites on cotton fabric for enhanced antimicrobial properties. In a typical synthesis, sericin was extracted by boiling raw silk in hot water and then nano-TiO_2 was dispersed in it which was further applied to cotton fabric with or without cross-linking agent by pad-dry-cure process. Antimicrobial property of modified cotton was estimated against gram-positive and gram-negative bacteria. The treated fabric showed more effective results against *S. aureus* than *E. coli* (Doakhan et al. 2013). Adnan and Moses developed UV-resistant fabrics by coating TiO_2 on silk/lyocell union fabrics. The results showed that TiO_2 as a UV finish significantly improve the UV absorbing activity of treated fabrics. Samples treated with TiO_2 showed good fastness properties up to 25 washing cycles (Adnan and Moses 2013). Montazer et al. developed antimicrobial finish for wool fabric with silver-loaded nano-TiO_2 under UV irradiations in an ultrasonic bath. The synthesized nanocomposite was stabilized on surface of wool by cross-linking with citric acid. The results of antimicrobial activity showed that increasing concentration of Ag/TiO_2 nanocomposite enhances the antimicrobial performance of the treated fabrics. In addition, citric acid enhanced adsorption of Ag/TiO_2 on surface of wool to improve antimicrobial performance (Montazer et al. 2011a). Guo et al. synthesized anatase TiO_2 nanotubes from TiO_2 powder in terms of the production of ROS and photocatalytic degradation of NDMA (N-nitrosodimethylamine) was evaluated. The synthesized nanotubes showed significantly higher NDMA degradation efficiency than nanopowder. The tubular morphology was responsible for higher NDMA removal because of its confinement effect leading to NDMA molecules within nanotube being attacked by ROS (Guo et al. 2015). Pistkova et al. investigated the photocatalytic degradation of five different β-blockers (acebutolol, propranolol, atenolol, nadolol, and metoprolol) by using immobilized TiO_2 as a

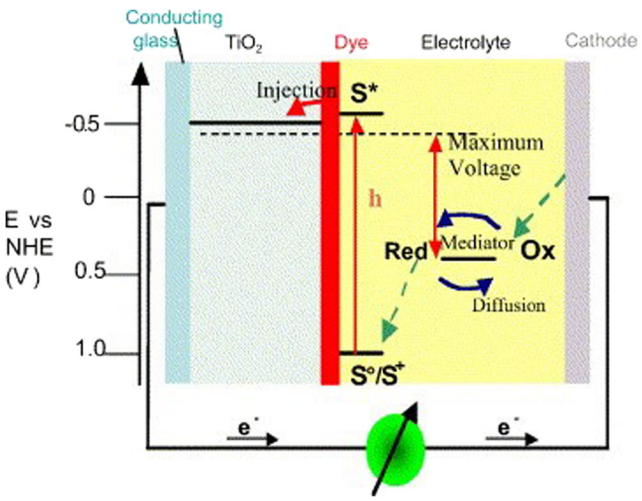

Fig. 29 Operating principle and energy level diagram of DSSC. Reprinted with permission from Grätzel (2004)). Copyright 2004, with permission from Elsevier

photocatalyst in an aqueous media. Evonik P90 and Degussa P25 were used for the synthesis of photocatalyst coatings on glass slides. The results showed that P25 exhibited higher photocatalytic activity compared to P90 as all β-blockers were completely degraded in 2 h (Píšťková et al. 2015). Dougna et al. studied photocatalytic degradation of phenol by using different commercial catalysts under laboratory reactor and UV-A lamp. The results described the best conditions for photocatalytic degradation of phenol when using Ahlstrom paper. In addition, P25 deposited glass showed the best phenol removal efficiency (Dougna et al. 2015). Ashraf et al. fabricated maghemite glass nanocomposite and use it for MB removal in wastewater treatments (Ashraf et al. 2018). In our previous study, we stabilized TiO_2 NPs onto cotton to increase the washing fastness and other functional properties of cotton fabric (Noman et al. 2018a).

Photovoltaic applications

The second most important use of TiO_2 NMs is in photovoltaics applications. Gratzel discussed heterojunction variants involved in the fabrication of DSSC (dye-sensitized solar cell) and investigated the perspectives for future development in DSSC. He sum up that DSSC have become a credible alternative to conventional p-n junction semiconductor devices (Grätzel 2003). In another review, Gratzel investigated the phenomenon behind the harvesting of solar energy into electrical energy by using nanocrystalline TiO_2 in DSSC. In a typical DSSC, a sensitizer is anchored on the surface of a semiconductor by which light is absorbed. At the interface, charge separation takes place from dye into the conduction band of semiconductor through photoinduced electron injection. Charge carriers are transported to the charge collector. Sensitizers with broader absorption band permits to harvest a large fraction of sunlight extended from UV to the near IR region. The operating principle of a DSSC is illustrated in Fig. 29 (Grätzel 2004). Perera et al. constructed a DSSC by depositing TiO_2 nanofilms on conductive glass plates sensitized with different dyes. The results revealed that for all three dyes, heterojunction produces photovoltaic response to light absorption. This method extended the spectral response range and increased the efficiency of DSSC (Perera et al. 2005).

Wu et al. utilized hydrothermal method to fabricate hierarchical anatase nano-TiO_2 comprised of ultra-thin nanosheets exposing high percentage (001) facets. The developed structures were utilized as a photoanode in QDSSC (quantum dot sensitized solar cells) with a power conversion efficiency of 3.47% (Wu et al. 2015). Xie et al. prepared an up-conversion luminescence electrode to fabricate DSSC by using TiO_2 (Er^{3+}, Yb^{3+}) powder under hydrothermal conditions. The prepared powder converts infrared light into visible light which the dye can easily absorb with wavelengths of 510–700 nm, resulting in an increase in the photocurrent of the DSSC. The maximum efficiency of 7.28% was achieved by DSSC with 1/3 of the ratio of TiO_2/luminescence powder in the luminescence layer (Xie et al. 2011). Gokilamani et al. prepared DSSC by using natural dyes due to their cheap production and eco-friendly properties. In a typical procedure, TiO_2 thin films were prepared by using a sol-gel method which were further sensitized by the dyes extracted from *Basella alba* rubra spinach having an absorption at about 665 nm. The XRD analysis confirms the formation of anatase nanocrystals. The prepared DSSC showed 0.70% working efficiency (Gokilamani et al. 2014). Tesfamichael et al. investigated the characterization of a DSSC electrode made by TiO_2 nanofilms. The results related to the optical properties of the DSSC were investigated which showed a decrease in transmittance and an increase in absorbance for dyeing times up to 8 h (Tesfmichael et al. 2003). Ferber and Luther prepared TiO_2 photoelectrode for DSSC in which particles are sintered together with particle size 10–30 nm. The computer simulations of light absorption and scattering showed an increase in absorption by optimizing the size of the TiO_2 NPs. The results of these simulations showed that a mixture of small particles provide effective surface and larger particles are effective light scatterers with a potential to enhance solar absorption significantly (Ferber and Luther 1998). Wang et al. reported a simultaneous production of electricity and hydrogen with simultaneous urban wastewater contaminants removal by a DSPC (dye-sensitized photoelectrochemical cell). Ag and AgCl NPs supported on chiral TiO_2 nanofibers were used as a photoanode in DSPC. The results showed that developed DSPC significantly degrade the wastewater effluents with 98% conversion of electricity to hydrogen (Wang et al. 2015b). Al-Alwami et al. investigated the effects of different solvents on the extraction of natural dyes and evaluate the higher dye adsorption on TiO_2 NPs. They sum up that all extracted dyes adsorbed well on the surface of TiO_2 as confirmed by FTIR (Fourier transform infrared spectroscopy). Moreover, the highest adsorption of dyes was achieved by mixing them with TiO_2 with methanol/water ratio 3:1. However, *Pandanus amaryllifolius* dye showed its maximum adsorption at 2:1 of ethanol/water ratio (Al-Alwani et al. 2015). Sayama et al. used different cyanine and merocyanine organic dyes to investigate the efficient sensitization on TiO_2 nanocrystalline electrodes by producing J_{SC} (short-circuit photocurrent) and η_{SUN} (solar light-to-power conversion efficiency). They sum up that η_{SUN} and J_{SC} were improved by simultaneous adsorption of different dyes on a TiO_2 electrode with maximum power conversion efficiency 3.1% (Sayama et al. 2003). Jang et al. modified the surface of TiO_2 photoelectrode through hydroxylation treatment with NH_4OH solution at temperature 70 °C for 6 h to enhance the dye adsorption and power conversion efficiency of DSSC. The results revealed that NH_4OH solutions provide hydroxyl groups on the surface of TiO_2. More concentration of NH_4OH

increasing the values of η_{SUN} and J_{SC} because the amount of adsorbed dye increased (Jang et al. 2013). Ito et al. reported the fabrication of TiO_2 thin film with having a solar light to electric power conversion efficiency over 10% for DSSC. The fabrication of photoelectrode was done by the variation of $TiCl_4$ in layers of nanocrystalline TiO_2 which induced mechanical strength and adhesion of TiO_2 layer. This novel method exerts a substantial influence on the overall parameters and performance of DSSC resulting in improvements in energy conversion efficiency. The schematic configuration of a DSSC is described in Fig. 30 (Ito et al. 2008).

Subramanian and Wang used TiO_2 in a hierarchal multilayer-structured photoelectrode for DSSC and the comparison was made with Degussa P25. The results showed a superior performance for multilayer-structured photoelectrode as compared to other three electrodes. The improvement was attributed to higher dye adsorption, higher current conversion efficiency because of more fraction of light scattering, and good charge transportation (Subramanian and Wang 2014). Gomez et al. prepared highly efficient nanocrystalline DSSC by incorporating sensitizer into sputter deposited TiO_2 films. They achieved 7% solar light to electrical power efficiency after a pyridine treatment which is almost similar to conventional cells prepared with colloidal TiO_2. They sum up that the integral J_{SC} for the sputter deposited TiO_2 films was higher and the dye incorporation was uniform (Gomez et al. 2000). Gu et al. reported an improvement in photoelectric conversion efficiency by coupling TiO_2 with SnO_2 under a modified FSP process. In a typical procedure, TiO_2 is sealed in SnO_2 and the recombination losses are effectively suppressed because of negative shift of the Fermi level. The prepared TiO_2–SnO_2 DSSC showed a photoelectric conversion efficiency 3.82%

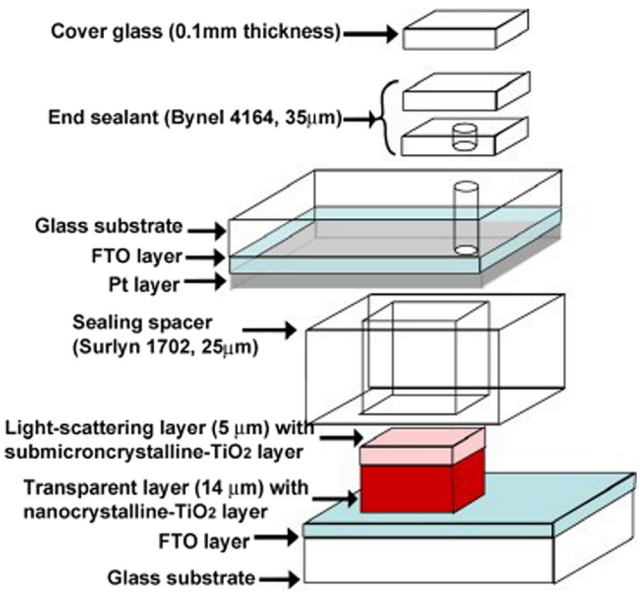

Fig. 30 Configuration of DSSC. Reprinted with permission from Ito et al. (2008)). Copyright 2008, with permission from Elsevier

which is significantly better than bare TiO_2 and SnO_2 devices. They sum up that photoelectric conversion efficiency could be further improved to 7.87% after surface modification (Gu et al. 2014). Liu et al. reported a novel synthesis of single crystalline TiO_2 nanorods by electrospinning and hydrothermal treatment to improve the light-harvesting and photovoltaic properties of DSSC. They explained that TiO_2 nanorods showed higher light utilization behavior as electron transfer received less resistance in TiO_2 nanorods than TiO_2 NPs. A thin layer of TiO_2 nanorods on TiO_2 NP working electrode significantly improved light-harvesting capacity and photoelectric conversion efficiency (Liu et al. 2015). Mashreghi and Ghasemi used a Pechini sol-gel process for the fabrication of TiO_2 NP pastes with different amounts of TTIP to investigate the effect of molar ratio on photovoltaic performance of DSSC. They sum up the results that with increasing amount of TTIP, the photovoltaic performance of DSSC was first increased and then decreased due to the microcracks in the mesoporous TiO_2 layers with high content of TTIP (Mashreghi and Ghasemi 2015). Barbe et al. prepared a novel DSSC based on photoelectrochemical method with nanocrystalline TiO_2 electrode. The light absorption was done by a sensitizer (monolayer of dye) that is adsorbed chemically on the surface of TiO_2. The obtained photovoltaic efficiency by using mesoporous nanofilms of anatase TiO_2 was almost 10% (Barbé et al. 1997). Wang et al. reviewed 1D (one-dimensional) TiO_2 nanostructures and their use in DSSC. They sum up the synthesis methods used for 1D TiO_2 nanostructures and their applications in DSSC. 1D TiO_2 nanostructures provide rapid and direct electron transfer which suggest them a promising choice for DSSC while conventional NP-based DSSC have several grain boundaries and surface defects that increase the electron recombination from photoanode to electrolyte (Wang et al. 2014a).

Summary

During the past decades, nano-TiO_2 have been intensively investigated in photocatalytic and photovoltaic fields due to its compatibility with current technologies. The continuous innovations in the fabrication of nano-TiO_2 have brought innovative properties in the up given fields with enhanced performance. In this thematic review, the main advantages of using nano-TiO_2 in photocatalytic and photovoltaic applications including self-cleaning coatings, self-sterilizing coatings, photodegradation of dyes, and DSSC have been discussed. The up given improvements have confirmed that nano-TiO_2 play a significant role in low-cost and efficient applications. In photocatalytic and photovoltaic applications, the generation, trapping, and transfer of charge carriers is a basic mechanism behind all photocatalytic processes which is closely connected with the properties of nano-TiO_2 as well as

its interface. However, the unique properties of nano-TiO_2 can be controlled through modification in size, crystal structure, and shape. We believe that high-quality and low-cost synthesis of nano-TiO_2 on large scale can be developed with more innovative applications besides the up given discussed fundamental achievements.

Compliance with ethical standards

Conflict of interest The authors declare that they have no conflict of interest.

References

Adnan M, Moses JJ (2013) Investigations on the effects of UV finishes using titanium dioxide on silk and lyocell union fabrics. J Text Appar Tech Managem 8(2):1–12

Afshar M, Badiei A, Eskandarloo H, Ziarani GM (2016) Charge separation by tetrahexahedron-$SrTiO_3$/TiO_2 heterojunction as an efficient photocatalyst. Res Chem Intermed 42:7269–7284

Al-Alwani MA, Mohamad AB, Kadhum AAH, Ludin NA (2015) Effect of solvents on the extraction of natural pigments and adsorption onto TiO_2 for dye-sensitized solar cell applications. Spectrochim Acta A 138:130–137

Anderson MA, Gieselmann MJ, Xu Q (1988) Titania and alumina ceramic membranes. J Membr Sci 39:243–258

Andersson M, Österlund L, Ljungström S, Palmqvist A (2002) Preparation of nanosize anatase and rutile TiO_2 by hydrothermal treatment of microemulsions and their activity for photocatalytic wet oxidation of phenol. J Phys Chem B 106:10674–10679

Anpo M, Shima T, Kodama S, Kubokawa Y (1987) Photocatalytic hydrogenation of propyne with water on small-particle titania: size quantization effects and reaction intermediates. J Phys Chem 91: 4305–4310

Arain RA, Khatri Z, Memon MH, Kim I-S (2013) Antibacterial property and characterization of cotton fabric treated with chitosan/AgCl–TiO_2 colloid. Carbohydr Polym 96:326–331

Arami H, Mazloumi M, Khalifehzadeh R, Sadrnezhaad S (2007) Sonochemical preparation of TiO_2 nanoparticles. Mater Lett 61: 4559–4561

Asahi R, Morikawa T, Irie H, Ohwaki T (2014) Nitrogen-doped titanium dioxide as visible-light-sensitive photocatalyst: designs, developments, and prospects. Chem Rev 114:9824–9852

Ashraf MA, Wiener J, Farooq A, Saskova J, Noman MT (2018) Development of maghemite glass fibre nanocomposite for adsorptive removal of methylene blue. Fibers Polym 19:1735–1746

Bai J, Zhou B (2014) Titanium dioxide nanomaterials for sensor applications. Chem Rev 114:10131–10176

Bai Y, Mora-Sero I, De Angelis F, Bisquert J, Wang P (2014) Titanium dioxide nanomaterials for photovoltaic applications. Chem Rev 114: 10095–10130

Banfield J (1998) Thermodynamic analysis of phase stability of nanocrystalline titania. J Mater Chem 8:2073–2076

Barbé CJ, Arendse F, Comte P, Jirousek M, Lenzmann F, Shklover V, Grätzel M (1997) Nanocrystalline titanium oxide electrodes for photovoltaic applications. J Am Ceram Soc 80:3157–3171

Barnard A, Curtiss L (2005) Prediction of TiO_2 nanoparticle phase and shape transitions controlled by surface chemistry. Nano Lett 5: 1261–1266

Barnard AS, Zapol P (2004) Effects of particle morphology and surface hydrogenation on the phase stability of TiO_2. Phys Rev B 70(1–13): 235403

Behnajady MA, Eskandarloo H (2015) Preparation of TiO_2 nanoparticles by the sol-gel method under different pH conditions and modeling of photocatalytic activity by artificial neural network. Res Chem Intermed 41:2001–2017

Behnajady M, Eskandarloo H, Modirshahla N, Shokri M (2011a) Investigation of the effect of sol-gel synthesis variables on structural and photocatalytic properties of TiO_2 nanoparticles. Desalination 278:10–17

Behnajady MA, Eskandarloo H, Modirshahla N, Shokri M (2011b) Sol-gel low-temperature synthesis of stable anatase-type TiO_2 nanoparticles under different conditions and its photocatalytic activity. Photochem Photobiol 87:1002–1008

Behzadnia A, Montazer M, Rashidi A, Mahmoudi Rad M (2014a) Rapid sonosynthesis of N-doped nano TiO_2 on wool fabric at low temperature: introducing self-cleaning, hydrophilicity, antibacterial/antifungal properties with low alkali solubility, yellowness and cytotoxicity. Photochem Photobiol 90:1224–1233

Behzadnia A, Montazer M, Rashidi A, Rad MM (2014b) Sonosynthesis of nano TiO_2 on wool using titanium isopropoxide or butoxide in acidic media producing multifunctional fabric. Ultrason Sonochem 21:1815–1826

Berger T, Sterrer M, Diwald O, Knözinger E, Panayotov D, Thompson TL, Yates JT (2005) Light-induced charge separation in anatase TiO_2 particles. J Phys Chem B 109:6061–6068

Bessekhouad Y, Robert D, Weber JV (2003) Synthesis of photocatalytic TiO_2 nanoparticles: optimization of the preparation conditions. J Photochem Photobiol A Chem 157:47–53

Blešić MD, Šaponjić Z, Nedeljković J, Uskoković D (2002) TiO_2 films prepared by ultrasonic spray pyrolysis of nanosize precursor. Mater Lett 54:298–302

Bourikas K, Kordulis C, Lycourghiotis A (2014) Titanium dioxide (anatase and rutile): surface chemistry, liquid–solid interface chemistry, and scientific synthesis of supported catalysts. Chem Rev 114: 9754–9823

Braginsky L, Shklover V (1999) Light absorption in TiO_2 nanoparticles. Eur Phys J D 9:627–630

Cai H, Mu W, Liu W, Zhang X, Deng Y (2015) Sol-gel synthesis highly porous titanium dioxide microspheres with cellulose nanofibrils-based aerogel templates. Inorg Chem Commun 51:71–74

Caratto V, Locardi F, Alberti S, Villa S, Sanguineti E, Martinelli A, Balbi T, Canesi L, Ferretti M (2016) Different sol-gel preparations of iron-doped TiO_2 nanoparticles: characterization, photocatalytic activity and cytotoxicity. J Sol-Gel Sci Technol 80:152–159

Cargnello M, Gordon TR, Murray CB (2014) Solution-phase synthesis of titanium dioxide nanoparticles and nanocrystals. Chem Rev 114: 9319–9345

Chae SY, Park MK, Lee SK, Kim TY, Kim SK, Lee WI (2003) Preparation of size-controlled TiO_2 nanoparticles and derivation of optically transparent photocatalytic films. Chem Mater 15:3326–3331

Chemseddine A, Moritz T (1999) Nanostructuring titania: control over nanocrystal structure, size, shape, and organization. Eur J Inorg Chem 1999:235–245

Chen X, Mao SS (2007) Titanium dioxide nanomaterials: synthesis, properties, modifications, and applications. Chem Rev 107:2891–2959

Chen H, Nanayakkara CE, Grassian VH (2012) Titanium dioxide photocatalysis in atmospheric chemistry. Chem Rev 112:5919–5948

Chibac AL, Melinte V, Buruiana T, Mangalagiu I, Buruiana EC (2015) Preparation of photocrosslinked sol-gel composites based on urethane-acrylic matrix, silsesquioxane sequences, TiO_2, and Ag/Au nanoparticles for use in photocatalytic applications. J Polym Sci A Polym Chem 53:1189–1204

Choi W, Termin A, Hoffmann MR (1994) The role of metal ion dopants in quantum-sized TiO_2: correlation between photoreactivity and charge carrier recombination dynamics. J Phys Chem 98:13669–13679

Cölfen H, Antonietti M (2005) Mesocrystals: inorganic superstructures made by highly parallel crystallization and controlled alignment. Angew Chem Int Ed 44:5576–5591

Coppens P, Chen Y, Trzop EB (2014) Crystallography and properties of polyoxotitanate nanoclusters. Chem Rev 114:9645–9661

Cot F, Larbot A, Nabias G, Cot L (1998) Preparation and characterization of colloidal solution derived crystallized titania powder. J Eur Ceram Soc 18:2175–2181

Dahl M, Liu Y, Yin Y (2014) Composite titanium dioxide nanomaterials. Chem Rev 114:9853–9889

De Angelis F, Di Valentin C, Fantacci S, Vittadini A, Selloni A (2014) Theoretical studies on anatase and less common TiO_2 phases: bulk, surfaces, and nanomaterials. Chem Rev 114:9708–9753

Diebold U (2003) The surface science of titanium dioxide. Surf Sci Rep 48:53–229

Doakhan S, Montazer M, Rashidi A, Moniri R, Moghadam M (2013) Influence of sericin/TiO_2 nanocomposite on cotton fabric: part 1. Enhanced antibacterial effect. Carbohydr Polym 94:737–748

Dominguez R, Alarcón-Flores G, Aguilar-Frutis M, Sánchez-Alarcón R, Falcony C, Dorantes-Rosales H, González-Velázquez J, Rivas-López D (2016) Effect on the stabilization of the anatase phase and luminescent properties of samarium-doped TiO_2 nanocrystals prepared by microwave irradiation. J Alloys Compd 687:121–129

Dong R, Jiang S, Li Z, Chen Z, Zhang H, Jin C (2015) Superhydrophilic TiO_2 nanorod films with variable morphology grown on different substrates. Mater Lett 152:151–154

Dougna AA, Gombert B, Kodom T, Djaneye-Boundjou G, Boukari SO, Leitner NKV, Bawa LM (2015) Photocatalytic removal of phenol using titanium dioxide deposited on different substrates: effect of inorganic oxidants. J Photochem Photobiol A Chem 305:67–77

El-Roz M, Haidar Z, Lakiss L, Toufaily J, Thibault-Starzyk F (2013) Immobilization of TiO_2 nanoparticles on natural Luffa cylindrica fibers for photocatalytic applications. RSC Adv 3:3438–3445

El-Shafei A, ElShemy M, Abou-Okeil A (2015) Eco-friendly finishing agent for cotton fabrics to improve flame retardant and antibacterial properties. Carbohydr Polym 118:83–90

Eskandarloo H, Badiei A, Behnajady MA, Ziarani GM (2014) Minimization of electrical energy consumption in the photocatalytic reduction of Cr (VI) by using immobilized Mg, Ag co-impregnated TiO_2 nanoparticles. RSC Adv 4:28587–28596

Eskandarloo H, Badiei A, Behnajady MA, Ziarani GM (2015) Ultrasonic-assisted sol-gel synthesis of samarium, cerium co-doped TiO_2 nanoparticles with enhanced sonocatalytic efficiency. Ultrason Sonochem 26:281–292

Eskandarloo H, Badiei A, Behnajady MA, Tavakoli A, Ziarani GM (2016) Ultrasonic-assisted synthesis of Ce doped cubic–hexagonal $ZnTiO_3$ with highly efficient sonocatalytic activity. Ultrason Sonochem 29:258–269

Eskandarloo H, Zaferani M, Kierulf A, Abbaspourrad A (2018) Shape-controlled fabrication of TiO_2 hollow shells toward photocatalytic application. Appl Catal B 227:519–529

Fan Z, Meng F, Gong J, Li H, Ding Z, Ding B (2016) One-step hydrothermal synthesis of mesoporous Ce-doped anatase TiO_2 nanoparticles with enhanced photocatalytic activity. J Mater Sci Mater Electron (11):11866–11872

Fathy M, Hamad H, Kashyout AEH (2016) Influence of calcination temperatures on the formation of anatase TiO_2 nano rods with a polyol-mediated solvothermal method. RSC Adv 6:7310–7316

Fattakhova-Rohlfing D, Zaleska A, Bein T (2014) Three-dimensional titanium dioxide nanomaterials. Chem Rev 114:9487–9558

Feng X, Zhai J, Jiang L (2005) The fabrication and switchable superhydrophobicity of TiO_2 nanorod films. Angew Chem Int Ed 44:5115–5118

Ferber J, Luther J (1998) Computer simulations of light scattering and absorption in dye-sensitized solar cells. Sol Energy Mater Sol Cells 54:265–275

Fujishima A, Rao TN, Tryk DA (2000) Titanium dioxide photocatalysis. J Photochem Photobiol C: Photochem Rev 1:1–21

Fujishima A, Zhang X, Tryk DA (2008) TiO_2 photocatalysis and related surface phenomena. Surf Sci Rep 63:515–582

Gaminian H, Montazer M (2015) Enhanced self-cleaning properties on polyester fabric under visible light through single-step synthesis of cuprous oxide doped nano-TiO_2. Photochem Photobiol 91:1078–1087

Gedanken A (2004) Using sonochemistry for the fabrication of nanomaterials. Ultrason Sonochem 11:47–55

Ghanem A, Badawy A, Ismail N, Tian ZR, Rehim MA, Rabia A (2014) Photocatalytic activity of hyperbranched polyester/TiO_2 nanocomposites. Appl Catal A 472:191–197

Gokilamani N, Muthukumarasamy N, Thambidurai M, Ranjitha A, Velauthapillai D (2014) Basella alba rubra spinach pigment-sensitized TiO_2 thin film-based solar cells. Appl Nanosci 5:297

Gomez M, Lu J, Olsson E, Hagfeldt A, Granqvist C (2000) High efficiency dye-sensitized nanocrystalline solar cells based on sputter deposited Ti oxide films. Sol Energy Mater Sol Cells 64:385–392

Grätzel M (2003) Dye-sensitized solar cells. J Photochem Photobiol C: Photochem Rev 4:145–153

Grätzel M (2004) Conversion of sunlight to electric power by nanocrystalline dye-sensitized solar cells. J Photochem Photobiol A Chem 164:3–14

Gu F, Huang W, Wang S, Cheng X, Hu Y, Li C (2014) Improved photoelectric conversion efficiency from titanium oxide-coupled tin oxide nanoparticles formed in flame. J Power Sources 268:922–927

Guo W, Lin Z, Wang X, Song G (2003) Sonochemical synthesis of nanocrystalline TiO_2 by hydrolysis of titanium alkoxides. Microelectron Eng 66:95–101

Guo X, Li Q, Zhang M, Long M, Kong L, Zhou Q, Shao H, Hu W, Wei T (2015) Enhanced photocatalytic performance of N-nitrosodimethylamine on TiO_2 nanotube based on the role of singlet oxygen. Chemosphere 120:521–526

Gupta KK, Jassal M, Agrawal AK (2007) Functional finishing of cotton using titanium dioxide and zinc oxide nanoparticles. Res J Text Appar 11:1–10

Harifi T, Montazer M (2014) Fe^{3+}: Ag/TiO_2 nanocomposite: synthesis, characterization and photocatalytic activity under UV and visible light irradiation. Appl Catal A 473:104–115

He H-Y (2016) Facile synthesis of ultrafine CuS nanocrystalline/TiO_2: Fe nanotubes hybrids and their photocatalytic and Fenton-like photocatalytic activities in the dye degradation. Microporous Mesoporous Mater 227:31–38

He H-Y (2017a) Efficient hydrogen evolution activity of 1T-MoS_2/Si-doped TiO_2 nanotube hybrids. Int J Hydrog Energy 42:20739–20748

He H-Y (2017b) Facile synthesis of Bi_2S_3 nanocrystalline-modified TiO_2: Fe nanotubes hybrids and their photocatalytic activities in dye degradation. Part Sci Technol 35:410–417

He H-Y, Chen P (2012) Recent advances in property enhancement of nano TiO_2 in photodegradation of organic pollutants. Chem Eng Commun 199:1543–1574

He Z, He H (2011) Synthesis and photocatalytic property of N-doped TiO_2 nanorods and nanotubes with high nitrogen content. Appl Surf Sci 258:972–976

He H-Y, Tian C-Y (2016) Rapid photo- and photo-Fenton-like catalytic removals of malachite green in aqueous solution on undoped and doped TiO_2 nanotubes. Desalin Water Treat 57:14622–14631

He H-Y, He Z, Shen Q (2018) TiO_2: Si nanotube/1T-$MoSe_2$ nanosheet hybrids with highly efficient hydrogen evolution catalytic activity. J Colloid Interface Sci 522:136–143

Hebeish A, Abdelhady M, Youssef A (2013) TiO_2 nanowire and TiO_2 nanowire doped Ag-PVP nanocomposite for antimicrobial and self-cleaning cotton textile. Carbohydr Polym 91:549–559

Henderson MA, Lyubinetsky I (2013) Molecular-level insights into photocatalysis from scanning probe microscopy studies on TiO_2 (110). Chem Rev 113:4428–4455

Henglein A (1989) Small-particle research: physicochemical properties of extremely small colloidal metal and semiconductor particles. Chem Rev 89:1861–1873

Hossain MK, Akhtar US, Koirala AR, Hwang IC, Yoon KB (2015) Steam-assisted synthesis of uniformly mesoporous anatase and its remarkably superior photocatalytic activities. Catal Today 243:228–234

Hurum DC, Gray KA, Rajh T, Thurnauer MC (2005) Recombination pathways in the Degussa P_{25} formulation of TiO_2: surface versus lattice mechanisms. J Phys Chem B 109:977–980

Ito S, Murakami TN, Comte P, Liska P, Grätzel C, Nazeeruddin MK, Grätzel M (2008) Fabrication of thin film dye sensitized solar cells with solar to electric power conversion efficiency over 10%. Thin Solid Films 516:4613–4619

Jang I, Song K, Park J-H, Oh S-G (2013) Enhancement of dye adsorption on TiO_2 surface through hydroxylation process for dye-sensitized solar cells. Bull Kor Chem Soc 34:2883–2888

Jhuang Y-Y, Cheng W-T (2016) Fabrication and characterization of silver/titanium dioxide composite nanoparticles in ethylene glycol with alkaline solution through sonochemical process. Ultrason Sonochem 28:327–333

Jiu J, Isoda S, Adachi M, Wang F (2007) Preparation of TiO_2 nanocrystalline with 3–5 nm and application for dye-sensitized solar cell. J Photochem Photobiol A Chem 189:314–321

Kadam A, Dhabbe R, Kokate M, Gaikwad Y, Garadkar K (2014) Preparation of N doped TiO_2 via microwave-assisted method and its photocatalytic activity for degradation of malathion. Spectrochim Acta A 133:669–676

Kale R, Meena CR (2012) Synthesis of titanium dioxide nanoparticles and application on nylon fabric using layer by layer technique for antimicrobial property. Adv Appl Sci Res 3:3073–3080

Kalpagam S, Kannadasan T (2014) Preparation of titanium dioxide nanoparticles and its application in wastewater treatment. J Chem Biol Phy Sci 4:1936

Kapilashrami M, Zhang Y, Liu Y-S, Hagfeldt A, Guo J (2014) Probing the optical property and electronic structure of TiO_2 nanomaterials for renewable energy applications. Chem Rev 114:9662–9707

Karahaliloglu Z, Hacker C, Demirbilek M, Seide G, Denkbas EB, Gries T (2014) Photocatalytic performance of melt-electrospun polypropylene fabric decorated with TiO_2 nanoparticles. J Nanopart Res 16:1

Kobayashi M (2016) Synthesis and development of titania with controlled structures. J Ceram Soc Jpn 124:863–869

Kolen'ko YV, Maximov V, Burukhin A, Muhanov V, Churagulov B (2003) Synthesis of ZrO_2 and TiO_2 nanocrystalline powders by hydrothermal process. Mater Sci Eng C 23:1033–1038

Lee K, Mazare A, Schmuki P (2014) One-dimensional titanium dioxide nanomaterials: nanotubes. Chem Rev 114:9385–9454

Li M, Jiang Y, Ding R, Song D, Yu H, Chen Z (2013) Hydrothermal synthesis of anatase TiO_2 nanoflowers on a nanobelt framework for photocatalytic applications. J Electron Mater 42:1290–1296

Li D, Wang H, Jing W, Fan Y, Xing W (2014) Fabrication of mesoporous TiO_2 membranes by a nanoparticle-modified polymeric sol process. J Colloid Interface Sci 433:43–48

Liu L, Chen X (2014) Titanium dioxide nanomaterials: self-structural modifications. Chem Rev 114:9890–9918

Liu G, Yang HG, Pan J, Yang YQ, Lu GQ, Cheng H-M (2014a) Titanium dioxide crystals with tailored facets. Chem Rev 114:9559–9612

Liu K, Cao M, Fujishima A, Jiang L (2014b) Bio-inspired titanium dioxide materials with special wettability and their applications. Chem Rev 114:10044–10094

Liu X, Fang J, Gao M, Wang H, Yang W, Lin T (2015) Improvement of light harvesting and device performance of dye-sensitized solar cells using rod-like nanocrystal TiO_2 overlay coating on TiO_2 nanoparticle working electrode. Mater Chem Phys 151:330–336

Look JL, Zukoski C (1995) Colloidal stability and titania precipitate morphology: influence of short-range repulsions. J Am Ceram Soc 78:21–32

Ma Y, Wang X, Jia Y, Chen X, Han H, Li C (2014) Titanium dioxide-based nanomaterials for photocatalytic fuel generations. Chem Rev 114:9987–10043

Makwana NM, Tighe CJ, Gruar RI, McMillan PF, Darr JA (2016) Pilot plant scale continuous hydrothermal synthesis of nano-titania; effect of size on photocatalytic activity. Mater Sci Semicond Process 42:131–137

Mashreghi A, Ghasemi M (2015) Investigating the effect of molar ratio between TiO_2 nanoparticles and titanium alkoxide in Pechini based TiO_2 paste on photovoltaic performance of dye-sensitized solar cells. Renew Energy 75:481–488

Meskin PE, Ivanov VK, Barantchikov AE, Churagulov BR, Tretyakov YD (2006) Ultrasonically assisted hydrothermal synthesis of nanocrystalline ZrO_2, TiO_2, $NiFe_2O_4$ and $Ni_{0.5}Zn_{0.5}Fe_2O_4$ powders. Ultrason Sonochem 13:47–53

Mohammadi M, Fray D, Mohammadi A (2008) Sol–gel nanostructured titanium dioxide: controlling the crystal structure, crystallite size, phase transformation, packing and ordering. Microporous Mesoporous Mater 112:392–402

Montazer M, Behzadnia A, Pakdel E, Rahimi MK, Moghadam MB (2011a) Photo induced silver on nano titanium dioxide as an enhanced antimicrobial agent for wool. J Photochem Photobiol B Biol 103:207–214

Montazer M, Pakdel E, Behzadnia A (2011b) Novel feature of nano-titanium dioxide on textiles: antifelting and antibacterial wool. J Appl Polym Sci 121:3407–3413

Moritz T, Reiss J, Diesner K, Su D, Chemseddine A (1997) Nanostructured crystalline TiO_2 through growth control and stabilization of intermediate structural building units. J Phys Chem B 101:8052–8053

Mutuma BK, Shao GN, Kim WD, Kim HT (2015) Sol–gel synthesis of mesoporous anatase–brookite and anatase–brookite–rutile TiO_2 nanoparticles and their photocatalytic properties. J Colloid Interface Sci 442:1–7

Nawaz M, Miran W, Jang J, Lee DS (2017) One-step hydrothermal synthesis of porous 3D reduced graphene oxide/TiO_2 aerogel for carbamazepine photodegradation in aqueous solution. Appl Catal B 203:85–95

Noman MT, Ashraf MA, Jamshaid H, Ali A (2018a) A novel green stabilization of TiO_2 nanoparticles onto cotton. Fibers Polym 19:2268–2277

Noman MT, Militky J, Wiener J, Saskova J, Ashraf MA, Jamshaid H, Azeem M (2018b) Sonochemical synthesis of highly crystalline photocatalyst for industrial applications. Ultrasonics 83:203–213

Noman MT, Wiener J, Saskova J, Ashraf MA, Vikova M, Jamshaid H, Kejzlar P (2018c) In-situ development of highly photocatalytic multifunctional nanocomposites by ultrasonic acoustic method. Ultrason Sonochem 40:41–56

O'regan B, Gratzel M (1991) A low-cost, high-efficiency solar cell based on dye-sensitized colloidal TiO_2 films. Nature 353:737–740

Oskam G, Nellore A, Penn RL, Searson PC (2003) The growth kinetics of TiO_2 nanoparticles from titanium (IV) alkoxide at high water/titanium ratio. J Phys Chem B 107:1734–1738

Pang CL, Lindsay R, Thornton G (2013) Structure of clean and adsorbate-covered single-crystal rutile TiO_2 surfaces. Chem Rev 113:3887–3948

Perelshtein I, Applerot G, Perkas N, Grinblat J, Gedanken A (2012) A one-step process for the antimicrobial finishing of textiles with crystalline TiO_2 nanoparticles. Chem Eur J 18:4575–4582

Perera V, Pitigala P, Senevirathne M, Tennakone K (2005) A solar cell sensitized with three different dyes. Sol Energy Mater Sol Cells 85: 91–98

Pierre AC, Pajonk GM (2002) Chemistry of aerogels and their applications. Chem Rev 102:4243–4266

Píšťková V, Tasbihi M, Vávrová M, Štangar UL (2015) Photocatalytic degradation of β-blockers by using immobilized titania/silica on glass slides. J Photochem Photobiol A Chem 305:19–28

Prasad K, Pinjari D, Pandit A, Mhaske S (2010) Synthesis of titanium dioxide by ultrasound assisted sol–gel technique: effect of amplitude (power density) variation. Ultrason Sonochem 17:697–703

Qi K, Daoud WA, Xin JH, Mak C, Tang W, Cheung W (2006) Self-cleaning cotton. J Mater Chem 16:4567–4574

Qiu S, Kalita SJ (2006) Synthesis, processing and characterization of nanocrystalline titanium dioxide. Mater Sci Eng A 435:327–332

Rajh T, Dimitrijevic NM, Bissonnette M, Koritarov T, Konda V (2014) Titanium dioxide in the service of the biomedical revolution. Chem Rev 114:10177–10216

Roy AS, Parveen A, Koppalkar AR, Prasad MA (2010) Effect of nano-titanium dioxide with different antibiotics against methicillin-resistant Staphylococcus aureus. J Biomater Nanobiotechnol 1:37–41

Sadr FA, Montazer M (2014) In situ sonosynthesis of nano TiO_2 on cotton fabric. Ultrason Sonochem 21:681–691

Sakai N, Ebina Y, Takada K, Sasaki T (2004) Electronic band structure of titania semiconductor nanosheets revealed by electrochemical and photoelectrochemical studies. J Am Chem Soc 126:5851–5858

Sang L, Zhao Y, Burda C (2014) TiO_2 nanoparticles as functional building blocks. Chem Rev 114:9283–9318

Sarkar D, Chattopadhyay KK (2014) Branch density-controlled synthesis of hierarchical TiO_2 nanobelt and tunable three-step electron transfer for enhanced photocatalytic property. ACS Appl Mater Interfaces 6: 10044–10059

Sato H, Ono K, Sasaki T, Yamagishi A (2003) First-principles study of two-dimensional titanium dioxides. J Phys Chem B 107:9824–9828

Sattarfard R, Behnajady MA, Eskandarloo H (2018) Hydrothermal synthesis of mesoporous TiO_2 nanotubes and their adsorption affinity toward basic violet 2. J Porous Mater 25:359–371

Sayama K, Tsukagoshi S, Mori T, Hara K, Ohga Y, Shinpou A, Abe Y, Suga S, Arakawa H (2003) Efficient sensitization of nanocrystalline TiO_2 films with cyanine and merocyanine organic dyes. Sol Energy Mater Sol Cells 80:47–71

Schneider J, Matsuoka M, Takeuchi M, Zhang J, Horiuchi Y, Anpo M, Bahnemann DW (2014) Understanding TiO_2 photocatalysis: mechanisms and materials. Chem Rev 114:9919–9986

Senić Ž, Bauk S, Vitorović-Todorović M, Pajić N, Samolov A, Rajić D (2011) Application of TiO_2 nanoparticles for obtaining self-decontaminating smart textiles. Sci Technol Rev 61:63–72

Subramanian A, Wang H-W (2014) Hierarchical multilayer-structured TiO_2 electrode for dye-sensitized solar cells. J Photochem Photobiol A Chem 279:32–37

Sugimoto T, Okada K, Itoh H (1997) Synthetic of uniform spindle-type titania particles by the gel-sol method. J Colloid Interface Sci 193: 140–143

Sugimoto T, Zhou X, Muramatsu A (2003a) Synthesis of uniform anatase TiO_2 nanoparticles by gel-sol method: 3. Formation process and size control. J Colloid Interface Sci 259:43–52

Sugimoto T, Zhou X, Muramatsu A (2003b) Synthesis of uniform anatase TiO_2 nanoparticles by gel-sol method: 4. Shape control. J Colloid Interface Sci 259:53–61

Suslick KS (1986) Ultrasound in synthesis, modern synthetic methods 1986. Springer, pp 1–60

Szczepankiewicz SH, Colussi A, Hoffmann MR (2000) Infrared spectra of photoinduced species on hydroxylated titania surfaces. J Phys Chem B 104:9842–9850

Teoh WY, Mädler L, Beydoun D, Pratsinis SE, Amal R (2005) Direct (one-step) synthesis of TiO_2 and Pt/TiO_2 nanoparticles for photocatalytic mineralisation of sucrose. Chem Eng Sci 60:5852–5861

Teoh WY, Amal R, Mädler L, Pratsinis SE (2007) Flame sprayed visible light-active Fe-TiO_2 for photomineralisation of oxalic acid. Catal Today 120:203–213

Tesfmichael T, Will G, Bell J, Prince K, Dytlewski N (2003) Characterization of a commercial dye-sensitised titania solar cell electrode. Sol Energy Mater Sol Cells 76(1):25–35

Thompson TL, Yates JT (2006) Surface science studies of the photoactivation of TiO_2 new photochemical processes. Chem Rev 106:4428–4453

Uddin M, Cesano F, Bonino F, Bordiga S, Spoto G, Scarano D, Zecchina A (2007) Photoactive TiO_2 films on cellulose fibres: synthesis and characterization. J Photochem Photobiol A Chem 189:286–294

Ullattil SG, Periyat P (2015) Green microwave switching from oxygen rich yellow anatase to oxygen vacancy rich black anatase TiO_2 solar photocatalyst using Mn (ii) as 'anatase phase purifier'. Nanoscale 7: 19184–19192

Ullattil SG, Periyat P (2016) A 'one pot'gel combustion strategy towards Ti^{3+} self-doped 'black'anatase TiO^{2}−x solar photocatalyst. J Mater Chem A 4:5854–5858

Ullattil SG, Narendranath SB, Pillai SC, Periyat P (2018) Black TiO_2 nanomaterials: a review of recent advances. Chem Eng J 343:708–736

Valencia S, Vargas X, Rios L, Restrepo G, Marín JM (2013) Sol-gel and low-temperature solvothermal synthesis of photoactive nano-titanium dioxide. J Photochem Photobiol A Chem 251:175–181

Velhal S, Kulakrni S, Jaybhaye R (2014) Titanium dioxide nanoparticles for control of microorganisms. IJRCE 4

Wang L, Sasaki T (2014) Titanium oxide nanosheets: graphene analogues with versatile functionalities. Chem Rev 114:9455–9486

Wang N, Li J, Zhu L, Dong Y, Tang H (2008a) Highly photocatalytic activity of metallic hydroxide/titanium dioxide nanoparticles prepared via a modified wet precipitation process. J Photochem Photobiol A Chem 198:282–287

Wang P, Xie T, Peng L, Li H, Wu T, Pang S, Wang D (2008b) Water-assisted synthesis of anatase TiO_2 nanocrystals: mechanism and sensing properties to oxygen at room temperature. J Phys Chem C 112:6648–6652

Wang H, Guo Z, Wang S, Liu W (2014a) One-dimensional titania nanostructures: synthesis and applications in dye-sensitized solar cells. Thin Solid Films 558:1–19

Wang L, Cai Y, Song L, Nie W, Zhou Y, Chen P (2014b) High efficient photocatalyst of spherical TiO_2 particles synthesized by a sol-gel method modified with glycol. Colloids Surf A Physicochem Eng Asp 461:195–201

Wang X, Li Z, Shi J, Yu Y (2014c) One-dimensional titanium dioxide nanomaterials: nanowires, nanorods, and nanobelts. Chem Rev 114: 9346–9384

Wang B, de Godoi FC, Sun Z, Zeng Q, Zheng S, Frost RL (2015a) Synthesis, characterization and activity of an immobilized photocatalyst: natural porous diatomite supported titania nanoparticles. J Colloid Interface Sci 438:204–211

Wang D, Li Y, Puma GL, Wang C, Wang P, Zhang W, Wang Q (2015b) Dye-sensitized photoelectrochemical cell on plasmonic Ag/AgCl@ chiral TiO_2 nanofibers for treatment of urban wastewater effluents, with simultaneous production of hydrogen and electricity. Appl Catal B 168:25–32

Wei X, Cai H, Feng Q, Liu Z, Ma D, Chen K, Huang Y (2018) Synthesis of co-existing phases Sn-TiO_2 aerogel by ultrasonic-assisted sol-gel method without calcination. Mater Lett 228:379–383

Wiener J, Shahidi S, Goba M (2013) Laser deposition of TiO_2 nanoparticles on glass fabric. Opt Laser Technol 45:147–153

Wight A, Davis M (2002) Design and preparation of organic–inorganic hybrid catalysts. Chem Rev 102:3589–3614

Wu D, Long M, Zhou J, Cai W, Zhu X, Chen C, Wu Y (2009) Synthesis and characterization of self-cleaning cotton fabrics modified by TiO_2 through a facile approach. Surf Coat Technol 203:3728–3733

Wu W-Q, Lei B-X, Rao H-S, Xu Y-F, Wang Y-F, Su C-Y, Kuang D-B (2013) Hydrothermal fabrication of hierarchically anatase TiO_2 nanowire arrays on FTO glass for dye-sensitized solar cells. Sci Rep 3

Wu D, Zhang S, Jiang S, He J, Jiang K (2015) Anatase TiO_2 hierarchical structures composed of ultra-thin nano-sheets exposing high percentage {0 0 1} facets and their application in quantum-dot sensitized solar cells. J Alloys Compd 624:94–99

Xiao X, Liu X, Cao G, Zhang C, Xia L, Xu W, Xiao S (2015) Atomic layer deposition TiO_2/Al_2O_3 nanolayer of dyed polyamide/aramid blend fabric for high intensity UV light protection. Polym Eng Sci 55:1296–1302

Xie G, Lin J, Wu J, Lan Z, Li Q, Xiao Y, Yue G, Yue H, Huang M (2011) Application of upconversion luminescence in dye-sensitized solar cells. Chin Sci Bull 56:96–101

Xie Y, Xia C, Du H, Wang W (2015) Enhanced electrochemical performance of polyaniline/carbon/titanium nitride nanowire array for flexible supercapacitor. J Power Sources 286:561–570

Xue B, Sun T, J-k W, Mao F, Yang W (2015) AgI/TiO_2 nanocomposites: ultrasound-assisted preparation, visible-light induced photocatalytic degradation of methyl orange and antibacterial activity. Ultrason Sonochem 22:1–6

Yang J, Mei S, Ferreira J (2001) Hydrothermal synthesis of TiO_2 nanopowders from tetraalkylammonium hydroxide peptized sols. Mater Sci Eng C 15:183–185

Yang J, Mei S, Ferreira JM (2003) In situ preparation of weakly flocculated aqueous anatase suspensions by a hydrothermal technique. J Colloid Interface Sci 260:82–88

Yang J, Mei S, Ferreira JM (2004a) Hydrothermal processing of nanocrystalline anatase films from tetraethylammonium hydroxide peptized titania sols. J Eur Ceram Soc 24:335–339

Yang J, Mei S, Ferreira JMF (2004b) Hydrothermal fabrication of rod-like rutile nano-particles. Mater Sci Forum Trans Tech Publ 455-456:556–559

Yeung K, Lam Y (1983) A simple chemical vapour deposition method for depositing thin TiO_2 films. Thin Solid Films 109:169–178

Žabová H, Sobek J, Církva V, Šolcová O, Kment Š, Hájek M (2009) Efficient preparation of nanocrystalline anatase TiO_2 and V/TiO_2 thin layers using microwave drying and/or microwave calcination technique. J Solid State Chem 182:3387–3392

Zhang H, Banfield JF (2014) Structural characteristics and mechanical and thermodynamic properties of nanocrystalline TiO_2. Chem Rev 114:9613–9644

Zhang Q, Gao L (2003) Preparation of oxide nanocrystals with tunable morphologies by the moderate hydrothermal method: insights from rutile TiO_2. Langmuir 19:967–971

Zhang Z, Yates JT Jr (2012) Band bending in semiconductors: chemical and physical consequences at surfaces and interfaces. Chem Rev 112:5520–5551

Zhang Y, Li G, Jin Y, Zhang Y, Zhang J, Zhang L (2002) Hydrothermal synthesis and photoluminescence of TiO_2 nanowires. Chem Phys Lett 365:300–304

Zhang H, Zhu H, Sun R (2012) Fabrication of photocatalytic TiO_2 nanoparticle film on PET fabric by hydrothermal method. Text Res J 82: 747–754

Zheng Y, Lv K, Wang Z, Deng K, Li M (2012) Microwave-assisted rapid synthesis of anatase TiO_2 nanocrystals with exposed {0 0 1} facets. J Mol Catal A Chem 356:137–143

Zhou M, Yu J, Cheng B, Yu H (2005) Preparation and photocatalytic activity of Fe-doped mesoporous titanium dioxide nanocrystalline photocatalysts. Mater Chem Phys 93:159–163

Zhou W, Sun F, Pan K, Tian G, Jiang B, Ren Z, Tian C, Fu H (2011) Well-ordered large-pore mesoporous anatase TiO_2 with remarkably high thermal stability and improved crystallinity: preparation, characterization, and photocatalytic performance. Adv Funct Mater 21:1922–1930

Z-l L, Lindner E, Mayer HA (2002) Applications of sol–gel-processed interphase catalysts. Chem Rev 102:3543–3578

Znaidi L, Seraphimova R, Bocquet J, Colbeau-Justin C, Pommier C (2001) A semi-continuous process for the synthesis of nanosize TiO_2 powders and their use as photocatalysts. Mater Res Bull 36: 811–825